8.07f/W(Jul162004)
+model
CSR : 1536
Prod.Type:FTP
pp.1–26(col.fig.:f1–9,12,13)
ED:SowmyashreeTC
PAGN:mamatha SCAN:

ARTICLE IN PRESS

Available online at www.sciencedirect.com

ScienceDirect

ELSEVIER

Continental Shelf Research ▮ (▮▮▮▮) ▮▮▮–▮▮▮

CONTINENTAL SHELF RESEARCH

www.elsevier.com/locate/csr

Spatial flow and sedimentation patterns within patches of epibenthic structures

T.J. Bouma*, L.A. van Duren, S. Temmerman, T. Claverie, A. Blanco-Garcia, T. Ysebaert, P.M.J. Herman

Netherlands Institute of Ecology, P.O. Box 140, 4400 AC Yerseke, The Netherlands

Received 31 March 2005; received in revised form 5 December 2005; accepted 10 December 2005

Abstract

The objectives of the present study were twofold: (1) to identify spatial sedimentation and erosion patterns developing within patches of epibenthic structures (i.e. physical structures that protrude from the sediments, originating either from animals or plants) as a consequence of biophysical interactions; and (2) to assess the relevance of hydrodynamic flume studies for the long-term sediment dynamics in the field. We addressed these objectives by using patches of well-defined artificial structures (bamboo canes) for which we could easily monitor the long-term sediment dynamics in the field, measure the hydrodynamic effects in detail in the flume, and simulate the field and flume set-up with a commercially available hydrodynamic model. Two-year monitoring in the field showed that sedimentation was much larger in the high-density patches than the low-density ones. Within the high-density patches, comparable spatial patterns emerged at different field sites: erosion at the front and the side of the patches, and sedimentation more down-stream within the patches. The low-density patches showed no such patterns, and were generally characterised by some small-scale erosion directly around individual bamboo canes. Sedimentation and erosion in the field was well explained by the patterns in bed shear stress that were derived from our flume measurements. The 3D hydrodynamic modelling facilitated up-scaling of the flume results to the field, but failed to simulate accurately the effects at the leading edge. We conclude that: (A) field observations on sedimentation revealed interesting spatial patterns, but could not elucidate underlying processes; (B) detailed hydrodynamic measurements in a flume can elucidate these underlying processes, provided that appropriate scaling is being used; (C) flume studies are by definition not able to capture all spatial scales that are relevant for estuarine landscape formation and will always cause some flow artefacts; (D) hydrodynamic modelling offers a valuable tool to upscale flume observations, even though present models are not yet capable of fully reproducing all detailed spatial patterns; and (E) spatial heterogeneity is very important when looking at small-scale patches. There is a need for more spatially explicit and scale-dependent knowledge on bio-physical interactions.

Keywords: Ecosystem engineer; Epibenthic structure; Sediment dynamics; Hydrodynamics; Flume; Delft3D-FLOW model; Schelde estuary

1. Introduction

Estuaries are important systems from both an economical and ecological perspective. This has

*Corresponding author. Tel.: +31 0 113 577300; fax: +31 0 113 573616.
E-mail address: t.bouma@nioo.knaw.nl (T.J. Bouma).

0278-4343/$ - see front matter © 2007 Elsevier Ltd. All rights reserved.
doi:10.1016/j.csr.2005.12.019

Please cite this article as: Bouma, T.J., et al., Spatial flow and sedimentation patterns within patches of epibenthic structures, Continental Shelf Research (2007), doi:10.1016/j.csr.2005.12.019

resulted in a broad range of regulations to protect estuarine ecosystems (e.g. the RAMSAR convention [http://ramsar.org/], and the EU-birds and habitat directive [http://europa.eu.int/comm/environment/nature/legis.htm]). Protective management of these tidal ecosystems is complicated due to their dynamic character, with continuously changing currents, ongoing sedimentation and/or erosion processes, and complex feedback loops between abiotic and biotic factors. Reducing these dynamics is generally not a suitable management option, as the functioning and the ecological values of these tidal ecosystems usually depend strongly upon this dynamic character. Hence, management of such systems requires fundamental insight into the dynamic processes that govern sedimentation and erosion (sediment dynamics) on estuarine mudflats and saltmarshes (Bouma et al., 2005a, b; Temmerman et al., 2003, 2004; van de Koppel et al., 2005; van der Wal and Pye, 2004; van der Wal et al., 2002).

Estuarine ecosystems are governed by physical forces originating from tidal currents and wind generated waves, and by biophysical interactions between those forces and the organisms that inhabit the estuary. On the one hand, such physical forces have been shown to affect strongly the distribution of benthic fauna (Herman et al., 2001; Ysebaert et al., 2002), as well as the distribution of subtidal and intertidal plant species (De Leeuw et al., 1992; Houwing, 2000; van Katwijk and Hermus, 2000), and the sedimentation patterns within estuarine ecosystems (Allen, 2000; Widdows et al., 2004). On the other hand, many organisms that live within estuaries have been shown to be able to modify wave and tidal current motion (Bouma et al., 2005a, b; Widdows and Brinsley, 2002) and/or sediment stability (Friend et al., 2003a, b; Herman et al., 2001; Widdows and Brinsley, 2002; Widdows et al., 2004). Thus, within estuarine systems, organisms may affect sedimentation in two ways: *directly* and *indirectly*.

Direct effects of organisms on sedimentation may originate from altered erosion thresholds. Erosion thresholds of sediments may be reduced due to bioturbation (Blanchard et al., 1997; Widdows and Brinsley, 2002; Widdows et al., 2004), or increased by "gluing sediment with EPS" (Paterson, 1989; Paterson et al., 2000). Quantification of erosion thresholds is complicated and may be done by different methods, each with its own strengths and weaknesses. However, studies comparing different methods and field vs. lab measurements have enhanced our understanding of quantifying erosion thresholds (Tolhurst et al., 1999, 2000a, b; Widdows et al., this issue).

Indirect effects of organisms on sediment dynamics often originate from epibenthic structures that alter hydrodynamic forces from waves and currents, and to a lesser extent, from feeding currents of endobenthic animals such as cockles. We define epibenthic structures as physical structures that protrude from the sediments, and may originate either from animals or from plants. The presence of epibenthic structures will result in modified local flows, and thus in a modification of the erosive force that water exerts on the sediment (Friedrichs et al., 2000; Friedrichs, 2003). Well-known examples of organisms that create epibenthic structures comprise reef building fauna such as mussels and oysters, tube building worms such as *Lanice conchilega*, subtidal vegetation (e.g. seagrasses), and intertidal vegetation (e.g. seagrasses and many saltmarsh species).

Detailed hydrodynamic studies have been made for several of these epibenthic structure-forming organisms (Abelson et al., 1993; Allen, 2000; Koch, 2001; Madsen et al., 2001; Widdows and Brinsley, 2002; Wright et al., 1997). For practical reasons, there are some limitations to the available detailed hydrodynamic studies: (A) most studies have been carried out in flumes (for exceptions, see Bouma et al., 2005b; Koch and Gust, 1999; Leonard and Luther, 1995; Neumeier and Ciavola, 2004); (B) most studies lack direct measurements of the sediment dynamics (for exceptions, see Friedrichs, 2003; Koch, 1999; Neumeier and Ciavola, 2004; Shi et al., 2000); and (C) most studies lack spatially explicit information on patterns that may arise. On the other hand, most studies on sediment dynamics cover a larger temporal scale than most hydrodynamic studies, but often lack both detailed hydrodynamic measurements (Allen, 2000; Temmerman et al., 2003, 2004) and detailed information on fine-scale spatial patterns.

The objectives of the present study were twofold: (1) to identify spatial sedimentation and erosion patterns that emerge within patches of epibenthic structures, as a consequence of boundary layer development over and inside these structures; and (2) to determine the relevance of detailed hydrodynamic flume studies for long-term field observations on sediment dynamics on the bottom surface. To address these issues, we used patches of well-

Please cite this article as: Bouma, T.J., et al., Spatial flow and sedimentation patterns within patches of epibenthic structures, Continental Shelf Research (2007), doi:10.1016/j.csr.2005.12.019

defined artificial structures (bamboo canes) that could be placed easily both in the field and in the flume, and that could be described easily in a commercially available hydrodynamic model. We expected these bamboo patches to some extent to behave as a simplified model for patches of stiff marsh vegetation, e.g. *Spartina anglica* tussocks. In the field, we monitored sedimentation over a 2-year period, covering intertidal sites with different physical forcing and sediment characteristics. In the flume we performed a detailed hydrodynamic characterisation inside the patches, measuring vertical profiles from the leading to the trailing edge of the patch. With the hydrodynamic model, we simulated both the flume and the field set-up. These three data sets were subsequently compared and examined for spatial patterns inside the bamboo canopy.

2. Materials and methods

2.1. Field experiments

To assess the relevance of hydrodynamic flume studies to long-term sedimentation, we used artificial epibenthic structures as a simplified model system. These artificial epibenthic structures were constructed (January 2002) by pushing 0.5 m long bamboo sticks (6–8 mm diameter) 0.3 m into the sediment, leaving 0.2 m on top of the sediment. Patches with bamboo were circular and had a diameter of 2.2 m. We created patches with a high density (HD) of bamboo sticks (50 mm between neighbouring canes, 400 sticks m^{-2}), and with a low density (LD) (200 mm between neighbouring bamboo canes, 25 sticks m^{-2}). Bamboo patches were placed perpendicular to the direction of the current, which was determined from the ripple marks. That is, within individual patches, bamboo sticks were placed in rows parallel to the ripple marks, with succeeding rows shifted half the distance between individual canes (i.e., 25 mm shift in HD patches; 100 mm shift in LD patches).

2.1.1. Field site

The core of the experiment was carried out at the Molenplaat (51°26′N, 3°57′E), an intertidal flat in the middle of the Westerschelde estuary in the south west of the Netherlands (Fig. 1A). The elevation of this intertidal flat ranges between approximately −1 and +1 m relative to mean tidal level; the mean tidal range is approximately 5 m (Herman et al., 2001). During immersion, current velocities are around 0.2–0.3 m s^{-1}. The Molenplaat consists of two sites: a central, muddy part with fine sand that contains a high silt fraction; and a sandy part that contains medium sand with very little silt (Steyaert et al., 2001). 3 LD and 3 HD patches were placed in January 2002 at both the muddy and the sandy parts of the mudflat, as indicated in Fig. 1B. In addition to the bamboo patches at the Molenplaat, we also placed some HD patches in the vicinity of *Spartina* tussocks on mudflats that border salt-marshes (Fig. 1A). At the Paulina saltmarsh, 5 HD patches were placed in between *Spartina* tussocks in front of the marsh (Fig. 2C). This saltmarsh mudflat has a highly muddy character, and local hydrodynamics are described extensively in Bouma et al. (2005b). At the Valkenisseplaat, we placed 1 HD patch at a sandy site with *Spartina* tussocks (Fig. 2A and B), and 1 HD patch on the muddy site with *Spartina* tussocks.

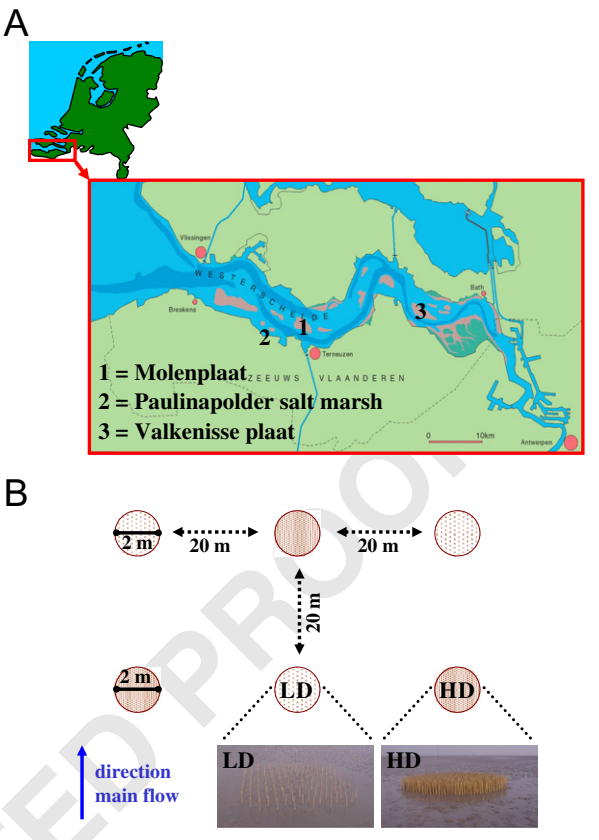

Fig. 1. (A) Map of the Schelde estuary, SW-Netherlands, indicating the locations where the artificial epibenthic structures were located; (B) schematic layout of the pattern in which the bamboo canes were placed at the Molenplaat.

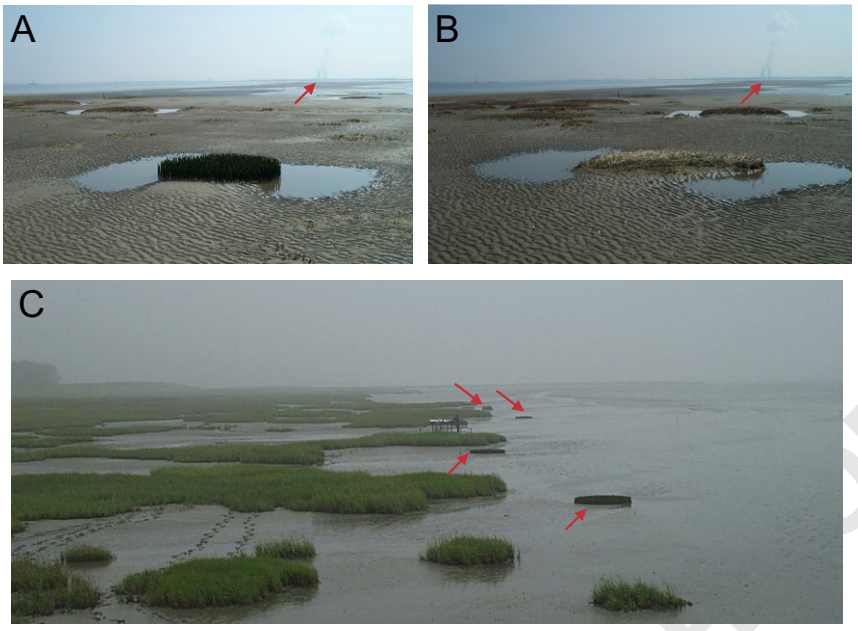

Fig. 2. Photo of a HD bamboo patch (A) and nearby *Spartina* tussock (B) at Valkenisseplaat during winter, illustrating the resemblance in channel development around both structures. The red arrows indicate the position of the Doel nuclear power plant (Belgium), and show that both photos were taken from a similar orientation. The direction of the main current is towards the downstream 'tail' of sediment behind the tussocks. (C) Photo of series of HD bamboo patches located in front of the Paullina marsh. The red arrows indicate the location of individual bamboo tussocks. The direction of the main current in varies with the tide (see Bouma et al., 2005b). During an tidal inundation cycle, the water flows: (1) perpendicular towards the marsh; (2) parallel to the marsh into the Westerschelde estuary (see Fig. 1); (3) parallel to the marsh out of the Westerschelde estuary; and (4) perpendicular away from the marsh. Highest flows occur during the first phase.

2.1.2. Sediment measurements in the artificial epibenthic structures

In the field, the height of the sediment was measured approximately bimonthly after placing the tussocks. Sediment accretion and/or erosion were quantified by laying a board on top of the bamboo canes, and measuring the distance between this board and the sediment. The length of the board allowed us to measure the topography both inside and around the bamboo patches with an accuracy of about 2 mm. Core samples (10 mm diameter, 20 mm deep) were taken 1 m outside the tussock as well as inside the tussock (June and August 2002). After freeze drying, the median grain size (μm) was determined with a laser particle sizer (Malvern Mastersizer 2000).

2.2. Flume experiments

2.2.1. Flume tank

Flow within bamboo patches was characterised in a large racetrack flume at the NIOO laboratory in Yerseke (see Bouma et al., 2005a). The flume consists of a large oval channel with a total length of 17.5 m, a straight working section of 10.8 m and a total capacity of about 9 m^3. The channel measures 0.6 m in cross section and water depth is maintained at 0.4 m. Water flow with a velocity up to 0.45 m s^{-1} is generated by a conveyor belt system, acting as a paddle wheel. The bends at either end of the flume have an outer diameter of 3.25 m. In these bends the water flow is guided through 4 sub-channels by turning vanes. Behind the conveyor belt and behind the bend at the start of the working section, the water passes through a stack of PVC tubes (Ø 20 mm) which act as collimators.

At the downstream end of the working section there is a 2 m long test section, with a transparent side window for direct observation, and a height-adjustable bottom that allows the placement of sediment down to a depth of 0.3 m, with the top of the sediment flush with the bottom of the working section of the flume. Within the test section, flow measurements were carried out with a Nortek® (field version) acoustic doppler velocimeter (ADV) set to operate at a rate of 25 Hz. The ADV was

Please cite this article as: Bouma, T.J., et al., Spatial flow and sedimentation patterns within patches of epibenthic structures, Continental Shelf Research (2007), doi:10.1016/j.csr.2005.12.019

mounted on a computerised 3D positioning system, which was mounted on a carriage that could be placed anywhere along the length of the working section. The 3D positioning system could move the ADV over the total width (y-axis) and depth (z-axis) of the flume and over a maximum length of 0.7 m in the direction of the main flow (x-axis). During all flow measurements, sufficient seeding was provided by adding small amounts of deep-sea clay sediment, which stays in suspension even at very low velocities.

Flow in flume tanks is always at best an idealised representation of flow in the field. Generally turbulence intensities are lower than in the field and the largest eddy sizes are determined by the dimensions of the tank. However, earlier work has indicated that properties of the boundary layer in the NIOO flume tank, as well as turbulence levels are very comparable to situations of steady flow in the field (Hendriks et al., 2006).

2.2.2. Velocity measurements within bamboo patches in the flume

The test section of the flume (2 m long × 0.6 m wide) was filled with a 0.1 m layer of sand, in which we placed 0.3 m long bamboo sticks (0.2 m length protruding into the water column). The bamboo densities were kept comparable to the field, using an interspacing of 50 and 200 mm for the high and low densities, respectively.

Vertical velocity profiles ($m\,s^{-1}$) were measured at several positions along a longitudinal transect. Velocity profiles were taken over a height of 20–300 mm from the sediment surface, and were determined for three different free-stream velocities (0.12, 0.25 and 0.37 $m\,s^{-1}$), i.e. the velocity range that represents field conditions (Bouma et al., 2005b). At each height, the measurements lasted 330 s yielding 8250 measurements, to enable calculation of turbulence parameters. Within the HD bamboo patches, the first measuring point was placed a few centimetres upstream of the leading edge of the bamboo, the next three within the bamboo tussock, and the fifth measuring point downstream of the bamboo patch. Within the LD bamboo patches, we measured vertical velocity profiles at seven x–y positions along a longitudinal transect. We also measured two sets of vertical velocity profiles: one set in close proximity to a bamboo stick (within about 30 mm); a second set inside the patch, but further removed away from the canes (about 100 mm).

Prior to processing, the ADV measurements were subjected to a filtering routine that removed data points with an average beam correlation lower than 60%. At individual measuring points in each profile we calculated the average of the three velocity components u, v and w. Subsequently, we estimated turbulent kinetic energy ($TKE = 0.5(\overline{u}^2 + \overline{v}^2 + \overline{w}^2)$; $m^2\,s^{-2}$) and the vertical momentum flux (Reynolds stress; $\overline{u'w'}$; $m^2\,s^{-2}$). The sign of this value indicates the direction of the momentum flux. In a Cartesian co-ordinate system negative values indicate momentum flux towards the bed. This is the predominant situation in a boundary layer with low velocities near the bed.

2.3. Model experiment

2.3.1. Model description

Flows were simulated for both the flume and field conditions. This was done using the commercially available Delft3D-FLOW model (www.wldelft.nl), which is a three-dimensional hydrodynamic model (Lesser et al., 2004; Temmerman et al., 2005). Below we give a brief description of the model. A full mathematical description is given by WL|Delft Hydraulics (2003).

The Delft3D-FLOW model computes flow characteristics (flow velocity, turbulence) dynamically in time over a three-dimensional spatial grid. The model is based on a finite-difference solution of the three-dimensional shallow-water equations with a k–ε turbulence closure model. The novel aspect of this flow model is that it accounts explicitly for the influence of rigid cylindrical structures (such as plant structures or other epibenthic structures) on drag and turbulence. The influence of cylindrical structures on drag leads, in the momentum equations, to an extra source term of friction force, $F(z)$ ($N\,m^{-3}$):

$$F(z) = \tfrac{1}{2}\rho_0\phi(z)n(z)|u(z)|u(z), \quad (1)$$

where ρ_0 is the the fluid density ($kg\,m^{-3}$); $\phi(z)$ the diameter of cylindrical structures (m) at height, z, above the bottom; $n(z)$ the number of structures per unit area (m^{-2}) at height z; $u(z)$ the horizontal flow velocity ($m\,s^{-1}$) at height z. The influence of cylindrical epibenthic structures on turbulence leads in the k–ε equations [Rodi, 1980] to (1) an extra source term of TKE, k ($m^2\,s^{-2}$):

Please cite this article as: Bouma, T.J., et al., Spatial flow and sedimentation patterns within patches of epibenthic structures, Continental Shelf Research (2007), doi:10.1016/j.csr.2005.12.019

$$\left(\frac{\partial k}{\partial t}\right)_{\text{cylinders}} = \frac{1}{1-A_p(z)}\frac{\partial}{\partial z}\left\{(1-A_p(z))(v+v_T/\sigma_k)\frac{\partial k}{\partial z}\right\} + T(z), \quad (2)$$

where $A_p(z) = (\pi/4)\ \phi^2(z)\ n(z) =$ the horizontal cross-sectional area of epibenthic structures per unit area at height z; v is the molecular fluid viscosity ($m^2\,s^{-1}$); v_T the eddy viscosity ($m^2\,s^{-1}$); σ_k the turbulent Prandtl–Schmidt number for self-mixing of turbulence ($\sigma_k = 1$); $T(z) = F(z)u(z)/\rho_0 =$ the work spent by the fluid ($m^2\,s^{-3}$) at height z; and (2) an extra source term of turbulent energy dissipation, ε ($m^2\,s^{-3}$):

$$\left(\frac{\partial \varepsilon}{\partial t}\right)_{\text{cylinders}} = \frac{1}{1-A_p(z)}\frac{\partial}{\partial z}\left\{(1-A_p(z))(v+v_T/\sigma_\varepsilon)\frac{\partial \varepsilon}{\partial z}\right\} + T(z)\tau_\varepsilon^{-1}, \quad (3)$$

where σ_ε is the turbulent Prandtl–Schmidt number for mixing of small-scale vorticity ($\sigma_\varepsilon = 1.3$); τ_ε the minimum of:

(1) the dissipation time scale of free turbulence:

$$\tau_{\text{free}} = \frac{1}{c_{2\varepsilon}}\left(\frac{k}{\varepsilon}\right) \quad \text{with coefficient } c_{2\varepsilon} = 1.96 \quad (4)$$

and (2) the dissipation time scale of eddies in between the cylindrical structures:

$$\tau_{\text{cylinders}} = \frac{1}{c_{2\varepsilon}\sqrt{c_\mu}}\left(\frac{L^2}{T}\right)^{1/3} \quad \text{with coefficient } c_\mu = 0.09, \quad (5)$$

where the eddies have a typical size limited by the smallest distance in between the cylindrical structures:

$$L(z) = C_l\left\{\frac{1-A_p(z)}{n(z)}\right\}^{1/2} \quad \text{with coefficient } C_l = 0.8. \quad (6)$$

This 3D plant–flow interaction model has been validated extensively against laboratory flume experiments (Baptist, unpublished results; Uittenbogaard, unpublished results) and against field data on flow patterns in saltmarshes (Temmerman et al., 2005).

2.3.2. Model application

The model was first applied to simulate flow characteristics in and above the bamboo patches in the flume experiments. A grid of 0.6 m (flume width) × 4 m (flume length) was used with a horizontal resolution of 0.1 × 0.1 m, and consisting of 10 vertical layers. A flat bottom and a constant water depth of 0.4 m were defined. Vertical rigid cylinders were defined over a section of 0.6 × 2 m, each with a cane diameter of 7 mm, height of 0.2 m and density of 400 and 25 m^{-2} for the high and LD patches, respectively. For each density, simulations were run for three different free-stream velocities (0.12, 0.25 and 0.37 $m\,s^{-1}$). The bottom roughness height was defined at 7×10^{-4} m, based on flow measurements in the flume without bamboo sticks. The horizontal eddy viscosity was estimated at $3 \times 10^{-5}\,m^2\,s^{-1}$, based on the grid resolution. We validated the simulated vertical profiles of flow velocity and TKE against the profiles that were measured at several places in the flume.

The model was subsequently applied to simulate flow characteristics in and above the bamboo patches in the field. A grid of 14 × 14 m was used, with the same horizontal and vertical resolution as for the flume simulations. Similarly, a flat bottom and constant water depth of 0.4 m was defined. A bamboo patch (with the same cane diameters, heights and densities as for the flume simulations) was defined over a circular region with a diameter of 2 × 2 m, and was placed in the centre of the 14 × 14 m grid. Simulations were run for a free-stream velocity of 0.37 $m\,s^{-1}$. The bottom roughness height was defined at 6 mm, based on an earlier field calibration of the flow model for the Paulina marsh study area (Temmerman et al., 2005). The horizontal eddy viscosity was kept the same as for the flume simulations. The spatial pattern of bed shear stress (τ_0), which was simulated within and around the bamboo patch, was used as a proxy for the simulated sedimentation and erosion patterns. Areas subject to high bed shear stress indicate areas of erosion, while areas subject to low bed shear stress indicate areas of sedimentation. The simulated patterns of bed shear stress were then compared against the field observations of sedimentation and erosion within and around the bamboo patches.

2.4. Comparison of experimental results and modelling data

In our flume and modelling experiments, we only focused on tidal currents, although we cannot exclude that wind generated waves may have affected sediment transport at the various field sites. Based on field observations at the Molenplaat, where we saw large sediment transport over a single tide in the absence of strong winds, we assumed tidal currents to be dominant.

Please cite this article as: Bouma, T.J., et al., Spatial flow and sedimentation patterns within patches of epibenthic structures, Continental Shelf Research (2007), doi:10.1016/j.csr.2005.12.019

In the modelling exercise, bed shear stress (τ_0) is used as a proxy to compare the sedimentation and erosion patterns found in the field. It is not always easy to estimate τ_0 directly from the ADV measurements. In a 'standard' turbulent boundary layer with a single logarithmic layer, there is a straightforward relationship between TKE, $\overline{u'w'}$ and the bed shear stress (τ_0):$\tau_0 = -\rho\overline{u'w'} = c_1\rho * (\text{TKE})$. Here c_1 is a constant (≈ 0.2) and ρ designates the density of (sea) water (Kim et al., 2000). These relationships are valid in situations where a log layer exists near the bed, and shear stress can be estimated by direct conversions (Thompson et al., 2003). However, in many situations where water is flowing over biogenic structures the link between these parameters is less straightforward (van Duren et al., 2006). This is also the case in the flow through a field of bamboo canes, where skimming flow is likely to occur over the canes. Although it is dangerous to derive absolute values of τ_0 from the ADV data, qualitatively there is still a strong relationship between near-bed turbulence and bed shear stress. We therefore assume that we can compare the spatial patterns of near-bed Reynolds stress to the spatial patterns of bed shear stress in the model.

3. Results

3.1. Field observations

Elevation measurements in the LD and HD bamboo patches at the Molenplaat, revealed a clear effect of bamboo density, orientation to the flow, and sediment type (or location) on sedimentation and erosion (Fig. 3). Sedimentation was much lower in the LD patches than in the HD patches. That is, regardless of sediment type, the HD patches revealed distinct patterns of sedimentation and erosion, whereas the elevation remained more constant at the LD patches. In the LD patches we observed only very small-scale erosion in the immediate vicinity of the bamboo sticks, but this had negligible effect on the average elevation level within the patch. Relative to the LD patches, the upstream front of the HD patches showed erosion from approx. 1 m before the patch to approx. 1 m into the patch (i.e. −2 to 0 m in Fig. 3A), whereas further downstream there was clear deposition. Relative to the LD patches, the HD patches also showed erosion at the sides of the patches that are orientated parallel to the main flow direction (i.e. the dip around −1 and 1 m in Fig. 3B). Sediment composition (or location) also had a clear effect on sedimentation, in that overall sediment accumulation was relatively large at the sandy site compared to the muddy site. Despite these differences, the spatial patterns of sedimentation and erosion were remarkably similar for both sediment types. The patterns also stood out in spite of temporal variation (see the appendix).

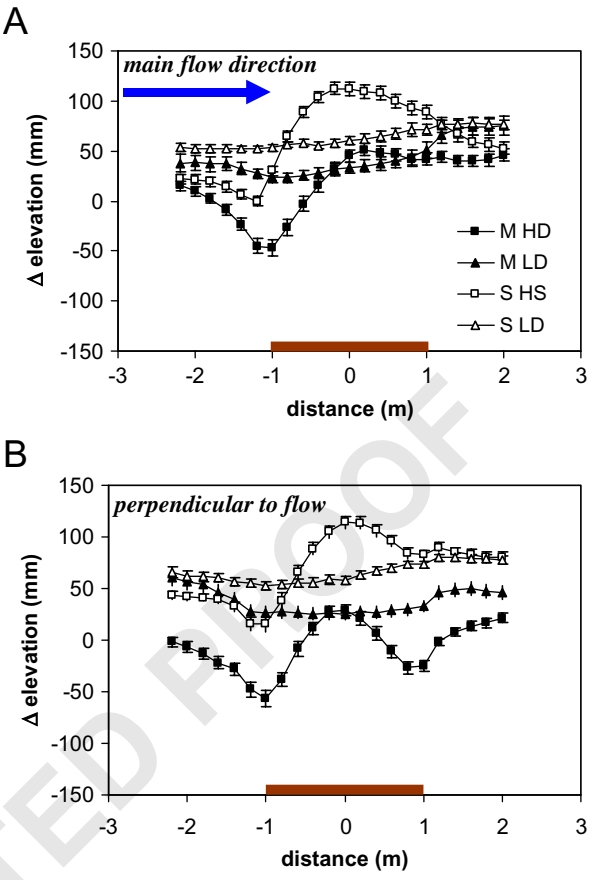

Fig. 3. Sedimentation and erosion in the low density (LD) and the high density (HD) bamboo patches at the muddy (M) and sandy (S) site of the Molenplaat. (A) Sedimentation and erosion along the central transect parallel to the main flow direction; (B) sedimentation and erosion along the central transect perpendicular to the main flow direction. Elevation 0 indicates the height of the sediment before the bamboo patch was placed. The bamboo patch was present between −1 and 1 m, as indicated by the line at the *x*-axis. Data points represent the average (±SE) over 3 replicate bamboo patches per treatment, for which the elevation was measured 11 times during 2002 and 2003 (6 March 2002; 21 March 2002; 11 April 2002; 1 May 2002; 28 May 2002; 27 June 2002; 29 July 2002; 21 October 2002; 10 March 2003; 15 July 2003 and 24 September 2003). (See Appendix for individual measurements).

Please cite this article as: Bouma, T.J., et al., Spatial flow and sedimentation patterns within patches of epibenthic structures, Continental Shelf Research (2007), doi:10.1016/j.csr.2005.12.019

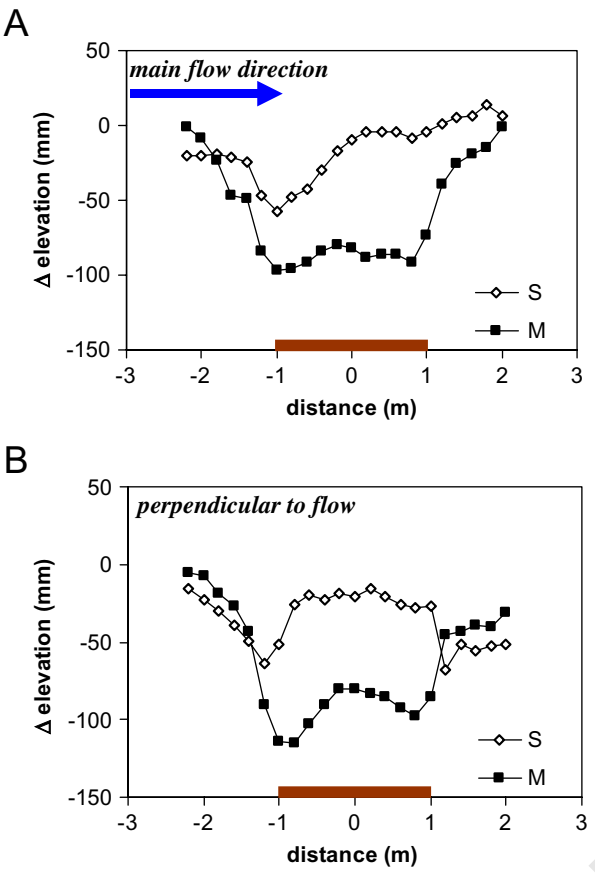

Fig. 4. Sedimentation and erosion in high density bamboo patches (HD) at the muddy (M) and the sandy (S) site of the Valkenisseplaat. (A) Sedimentation and erosion along the central transect parallel to the main flow direction; (B) sedimentation and erosion along the central transect perpendicular to the main flow direction . Elevation 0 indicates the height of the sediment before the bamboo patch was placed. The bamboo patch was present between −1 and 1 m, as indicated by the line at the *x*-axis. Data points represent the average over 4 repeated measurements at a single bamboo patch (8 July 2002; 4 September 2002; 22 April 2003; 24 September 2003).

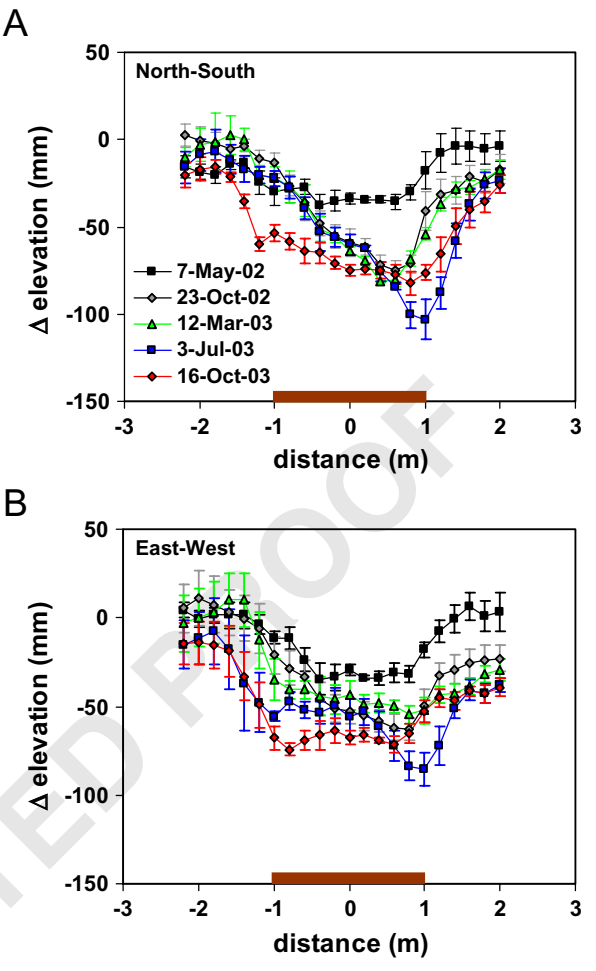

Fig. 5. Temporal variation in sedimentation and erosion in high density bamboo patches at Paulina polder saltmarsh. There was no clear indication on the main stream direction, so transects were orientated north-south (A) and east-west (B). Elevation 0 indicates the height of the sediment before the bamboo patch was placed. The bamboo patch was present between −1 and 1 m, as indicated by the line at the *x*-axis. Data points represent the average (±SE) over 5 replicate bamboo patches.

In contrast to the Molenplaat, where there appeared to be a tendency to net sediment accumulation both inside and around the LD and HD patches, there was an overall tendency to net erosion in the HD patches placed at both the Valkenisseplaat (Fig. 4) and the Paulina polder saltmarsh (Fig. 5). Erosion was particularly strong within these HD patches, whereas the area around the canes remained approximately level. This forms a distinct contrast with nearby tussocks of *Spartina anglica*, which tend to have a clear dome shape (Fig. 6). The discrepancy between bamboo patches and *Spartina* tussocks was remarkable, regarding their close resemblance when seen from a distance (Fig. 2A and B). The differences in patch dynamics between the *Spartina* and bamboo tussocks point at possible differences in hydrodynamic interaction between the stiff, relatively sparse bamboo, and the slightly flexible but much denser *Spartina* vegetation. The larger scale similarities of sedimentation and erosion around the perimeter of tussocks (Fig. 2A and B) could not be covered within the dimensions of our flume set-up.

Please cite this article as: Bouma, T.J., et al., Spatial flow and sedimentation patterns within patches of epibenthic structures, Continental Shelf Research (2007), doi:10.1016/j.csr.2005.12.019

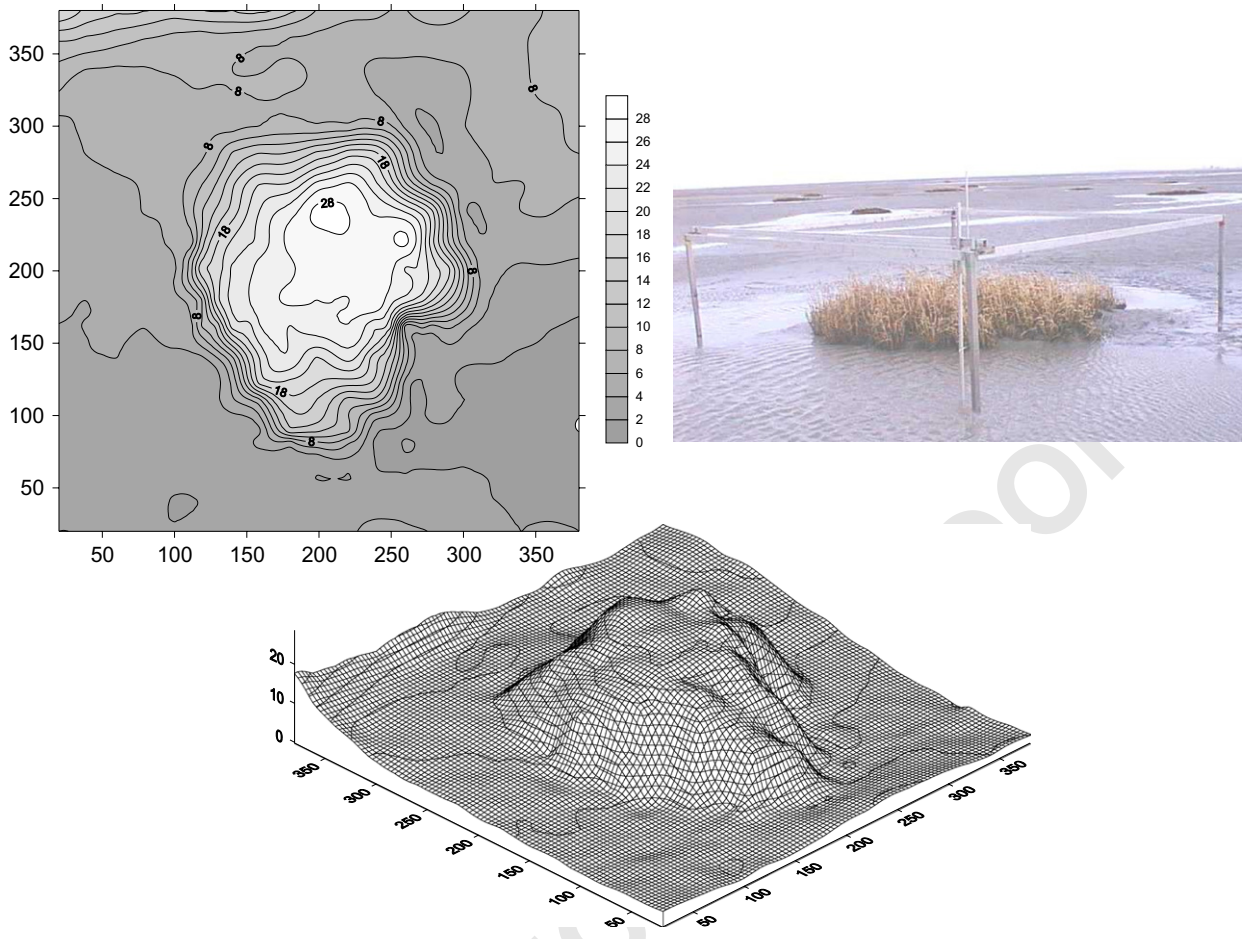

Fig. 6. Typical example of the dome shaped elevation pattern in *Spartina anglica* tussock.

Similar to the observations at the Molenplaat (Fig. 3), the muddy site at the Valkenisseplaat (Fig. 4) obtained a lower elevation than the sandy site, and the sandy site revealed similar spatial sedimentation and erosion patterns as the Molenplaat. The strongest erosion was observed at the upstream front of the HD patches (i.e. −2 to 0 m in Fig. 4A) and at the sides of the patches that are orientated parallel to the main flow direction (i.e. dip around −1 and 1 m in Fig. 4B). Lack of a dominant flow direction at the Paulina polder saltmarsh (details in legend Fig. 2), made it impossible to identify sedimentation patterns as clearly as observed at the Molenplaat (Fig. 3) and the Valkenisseplaat (Fig. 4). The overall loss of sediment within the bamboo patch was independent of temporal variation in elevation height at the mudflat, as reflected by the elevation measurements furthest away from the bamboo patch (Fig. 5). Temporal data suggest that the elevations and depressions in the level of the sediment develop relatively quickly, and remain relatively constant during subsequent periods. This quick response (visual observations showed response after a single tide) suggests that these patterns are caused initially by tidal currents, rather than by unpredictable wave events. However, we cannot exclude variations over time due to wind generated waves, and that this effect may vary among field sites.

At most sites, there was a tendency towards more coarse, median grain sizes within the bamboo patches (Table 1). However, this trend was not visible at the most muddy site (Paulina polder saltmarsh) and the Valkenisseplaat, where the sand was relatively coarse.

3.2. Flume measurements

The density of the bamboo canes had a strong effect on flow characteristics (Fig. 7). The HD patch

Please cite this article as: Bouma, T.J., et al., Spatial flow and sedimentation patterns within patches of epibenthic structures, Continental Shelf Research (2007), doi:10.1016/j.csr.2005.12.019

Table 1
The median grain size (μm) at the different field sites, both inside and outside the bamboo patches

Location substrate-type density bamboos	Molenplaat				Valkenisse		Paulinaploder
	Muddy HD	Muddy LD	Sandy HD	Sandy LD	Muddy HD	Sandy HD	Muddy HD
1 m outside tussock	100.3±7.88	71.6±3.6	155.0±3.49	172.3±11.6	88.5±0.015	182.5±0.53	50.3±2.45
Inside tussock	125.0±2.84	91.7±3.7	172.1±2.83	182.8±9.8	143.0+0.35	179.8±4.76	49.6±1.66
n	6	6	6	6	2	2	6

caused near skimming flow over the bamboo vegetation at all velocities and at nearly all distances from the leading edge (Fig. 7A–C). Below the canopy, particularly at lower velocities, there was little increase in velocity from the bed towards the top of the canes. Above the canopy, a clear boundary layer with a very steep gradient developed. At lower velocities, this boundary layer on top of the canopy developed earlier than at the high velocity. Both in relative and in absolute terms the flow reduction was greater at the higher velocity. At the trailing end of the canopy, the near-bed velocities at the high-velocity treatment were very close to zero, and considerably lower than in the lower velocities. Similar effects were also visible in the LD canopy, although here the profiles differed more conspicuously from true skimming flow (Fig. 7D–I). Inside the canopy there was a clear velocity gradient from the bed to the top of the canopy, but the biggest velocity increase was at the top of the canopy. There was also considerable horizontal heterogeneity in the flow. Measurements near the bamboo canes (Fig. 7D–F) showed lower velocities and a clearer separation in flow between canopy and overlying water than those taken as far away from the bamboo sticks as possible (Fig. 7G–I). However, the canes occupied only 0.13% of the total surface area within the LD patch. Although we have no intermediate measurements between 30 and 100 mm distance from the canes, we expect the latter situation (Fig. 7G–I) to be the most representative for the average flow through the patch.

As expected, the canes had clear effects on the turbulence structure inside and above the bamboo patches (Fig. 8), which correspond closely with measurements made by Neumeier (this volume). The effect differed widely between the two experimental densities. Within the LD patch the effect also differed between measurements in close proximity of a bamboo cane, and measurements further away. In the HD patch (Fig. 8A–C), very high levels of TKE were generated at the leading edge of the bamboo patches at the tips of the canes, i.e. at the location where the water hits the bamboo with the highest velocity. At low and intermediate velocities, other areas of relatively high turbulence are found at the trailing edge of the "meadow", just above the canopy, i.e. inside the steepest velocity gradient. At the highest velocity there was an area of elevated turbulence downstream of the patch. In the LD patch, turbulence was clearly elevated in the direct vicinity of the bamboo canes, regardless of the location within the patch (Fig. 8D–F). Highest levels still occurred at the leading edge of the patch but, at all velocities, turbulence remained relatively high inside the canopy. At greater distance from the canes (Fig. 8G–I), turbulence levels were still slightly elevated compared to levels outside the canopy, but clearly much lower than close to the canes (Fig. 8D–F). At the intermediate and highest velocity, highest TKE levels were measured near the bed.

Most interesting with regard to sedimentation and erosion processes are the profiles of vertical momentum flux ($\overline{u'w'}$). Both in the HD patch and in the LD patch in close proximity to the bamboo canes, values for $\overline{u'w'}$ were positive at the leading edge at the top of the canopy, indicating momentum transport upwards, into the water column. All other areas showed the "normal" downward momentum flux towards the sediment bed, in line with the direction of the local velocity gradients. In particular, the HD patch showed peak values at the top of the canopy (Fig. 9A–C). Inside the canopy, Reynolds stress values were generally low at the bed. Elevated Reynolds stress values were found only at the sediment water interface at the very front of the HD patch. In the LD patch the situation was quite different (Fig. 9D–I). Highest values of $\overline{u'w'}$ were always found near the bed. This effect was more pronounced in close proximity to the bamboo canes (Fig. 9D–F) than further away (Fig. 9G–I),

Please cite this article as: Bouma, T.J., et al., Spatial flow and sedimentation patterns within patches of epibenthic structures, Continental Shelf Research (2007), doi:10.1016/j.csr.2005.12.019

with the latter situation most likely being representative for the majority of the area within the bamboo patch. Inside the canopy, the levels of Reynolds stress at the sediment water interface were considerably lower in the HD patch than in the LD situation. However, levels at the bed at the leading edge were higher in the HD patch. This appeared to tie in nicely with the sedimentation and erosion

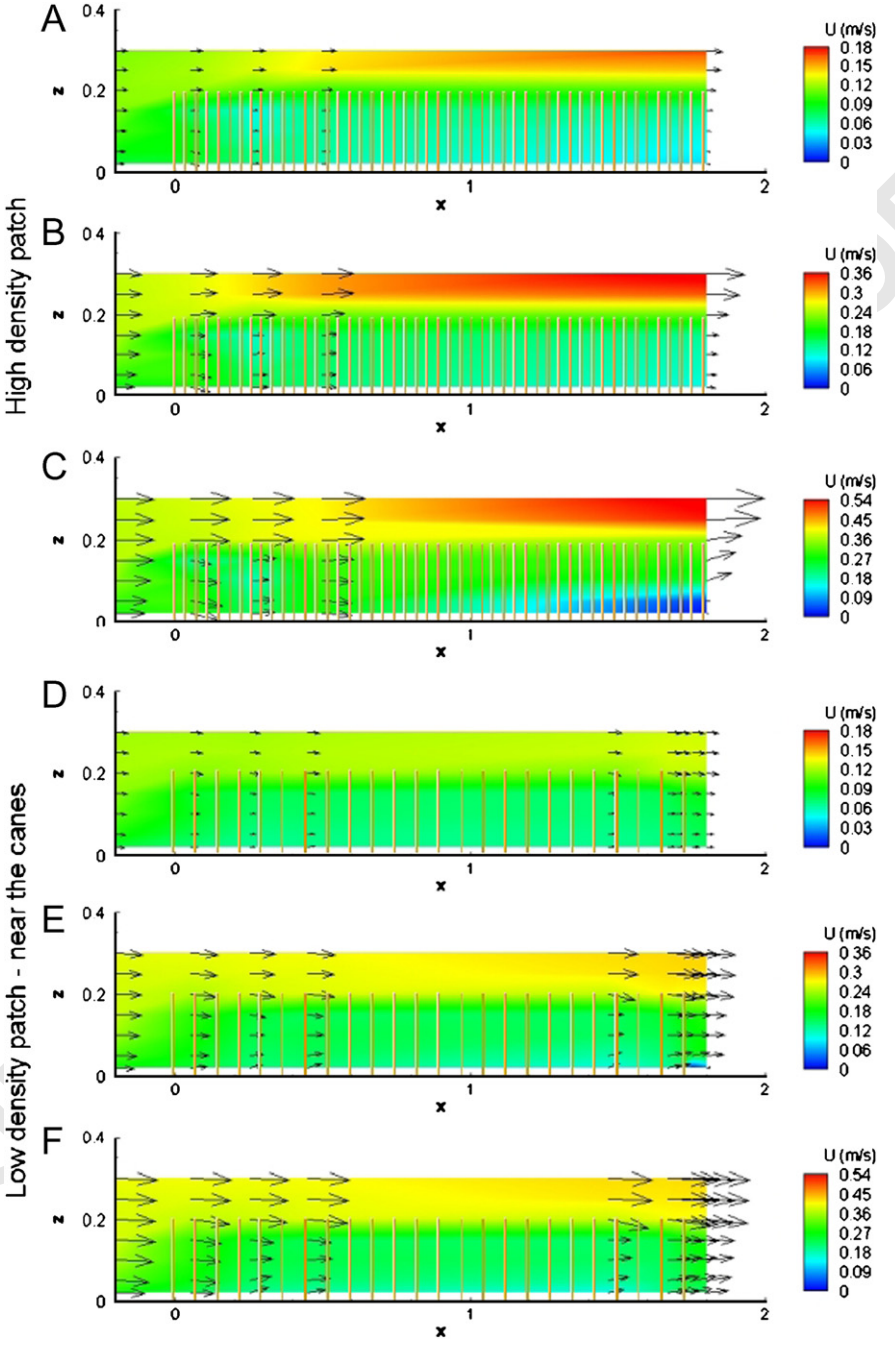

Fig. 7. Velocity profiles ($m\,s^{-1}$) measured at different positions in bamboo patches in the flume. (A–C): High density patch at low, intermediate, and high velocities, respectively. (D–F): Low density patch in close proximity to the bamboo canes. Velocities as per (A–C). (G–I): Low density patch away from the bamboo canes. The extent of the bamboo patch is indicated.

Please cite this article as: Bouma, T.J., et al., Spatial flow and sedimentation patterns within patches of epibenthic structures, Continental Shelf Research (2007), doi:10.1016/j.csr.2005.12.019

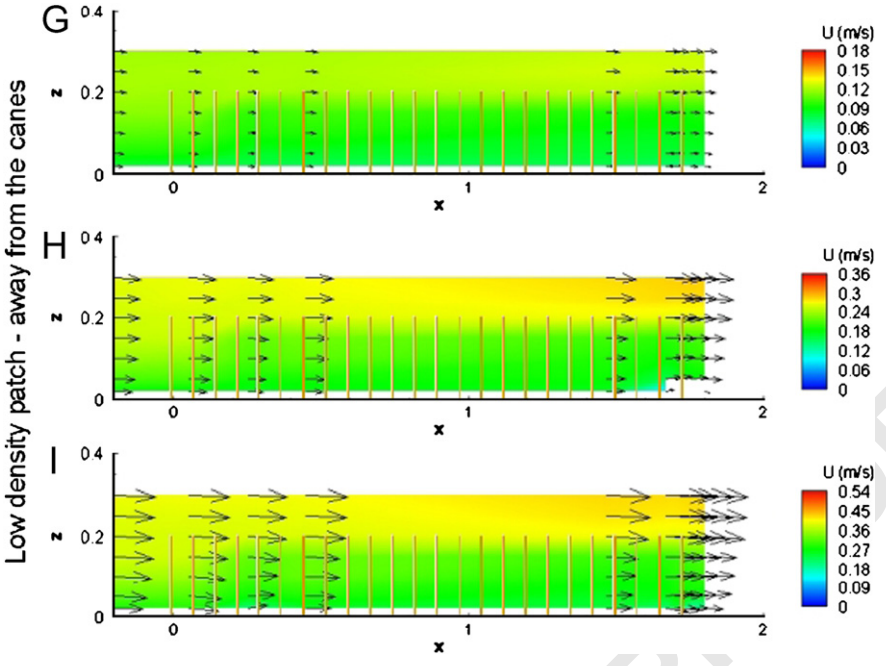

Fig. 7. (*Continued*)

patterns we observed in our field experiments. These data showed highest levels of erosion at the leading edge of HD patches, and relative sedimentation downstream. The elevated Reynolds stress close to the bamboo canes inside the LD patch in the flume also matches the field observation of small-scale erosion directly around individual canes.

In the experiments with the HD patch, all measurements were taken either in front of or inside the bamboo patch. In the experiments with the LD bamboo, some measurements were also taken behind the trailing edge. Over the course of the measurements some sedimentation took place in this area. This probably caused some interference of the elevated bottom with the lowest ADV measurements behind the bamboo. The high levels of TKE and Reynolds stress in this area should therefore be treated with caution.

3.3. Model results

3.3.1. Flume simulations

Comparison of Delft-3D simulated and flume-measured vertical profiles of flow velocity (u) and TKE revealed a fairly good correspondence between the model simulations and the flume measurements (Figs. 10 and 11). The model proved capable of reproducing the general features of the measured flow. In accordance with the flume data, the model predicted that flow velocities were reduced within the bamboo patch (due to the friction caused by the bamboo canes) and that the water was forced to flow at increased velocities above the bamboo patch. The simulated values of the flow velocities as well as the TKE were found to be of a very similar order of magnitude as our measurements. The model had a resolution of 10×10 cm, which was too coarse to resolve spatial differences in the flow at different distances from individual canes, as we measured in our LD patch. Inside the LD patch (Figs. 10B and 11B) the model results tended to fall neatly in between the data measured near the sticks and those measured further away from the canes. There were, however, some differences in the details. The flume experiments on the HD patch clearly showed high TKE values (Fig. 11A) and consequently a reduction in flow velocity (Fig. 10A) at the top of the canopy on the leading edge. In the modelled flume canopy, this phenomenon appeared to occur much further downstream of the leading edge. This discrepancy between measured and modelled data was largest at the HD patch. However, also in the LD patch we saw a much clearer separation between flow through the canopy

Please cite this article as: Bouma, T.J., et al., Spatial flow and sedimentation patterns within patches of epibenthic structures, Continental Shelf Research (2007), doi:10.1016/j.csr.2005.12.019

and the overlying water, than was simulated by the model.

3.3.2. Field simulations

The model simulations for the field situation also showed that the flow velocity is reduced within the circular bamboo patch and increased above the patch (Fig. 10). However, this effect was not so pronounced for the circular patch in the field as for the bamboo patch in the flume. The reason for this discrepancy lies in a different amount of free space next to the bamboo patch. In our (simulated) flume

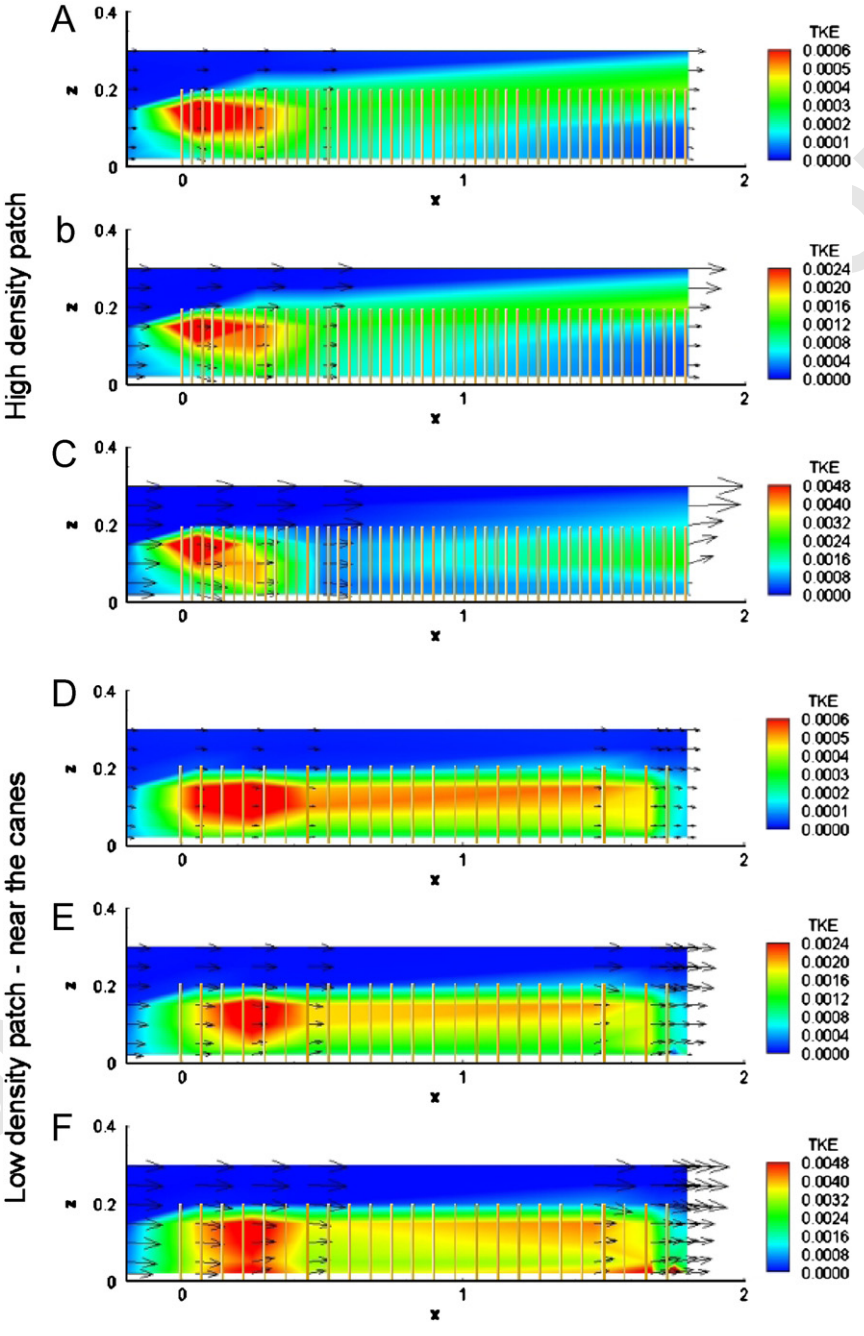

Fig. 8. (A–I) TKE profiles ($m^2 s^{-2}$) measured at different positions in bamboo patches in the flume. Patch densities and velocities as in Fig. 7.

Please cite this article as: Bouma, T.J., et al., Spatial flow and sedimentation patterns within patches of epibenthic structures, Continental Shelf Research (2007), doi:10.1016/j.csr.2005.12.019

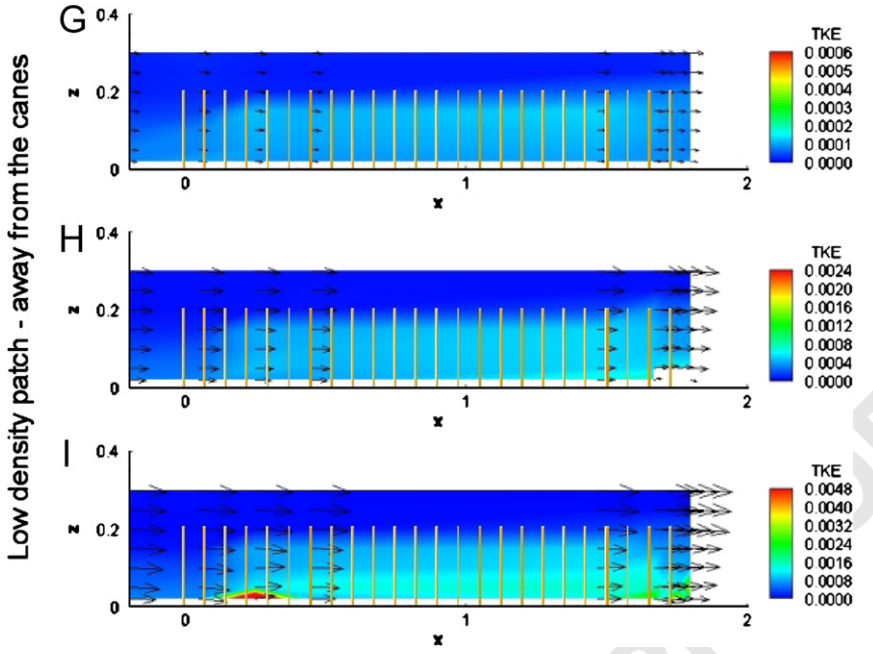

Fig. 8. (*Continued*)

set-up, the flume was filled with bamboo canes over its whole width, so that the water was forced to flow at higher velocities above and through the patch. In our (simulated) field set-up with free-standing circular patches, the water could also flow around the bamboo patch, resulting in increased flow velocities lateral to the bamboo patch. As a result, the model predicts a lesser increase in velocity above the field patch than in the flume (Fig. 10). As the predicted reduction of flow inside the canopy was also not as severe for the field as for the flume (Fig. 10), the velocity gradient between the tips of the bamboo canes and the overlying free-flowing water was considerably greater in flume simulations than in field simulations. Consequently, the model predicted that the generation of turbulence at the top of the canopy, at some distance downstream of the leading edge, was higher in the flume than in the field (Fig. 11). Thus, although the velocities in the simulations for the field and the flume patch were rather comparable, the model predicted somewhat higher levels of turbulence inside and just above the canopy, particularly in the LD patch.

The modelled patterns of bed shear stress (τ; $N\,m^{-2}$) were then used as a proxy for sedimentation and erosion patterns around the circular bamboo patch. In agreement with the field and flume observations, the differences in bed shear stress (τ) were much less pronounced in the LD patch than in the HD patch (Fig. 12; note scale difference between Fig. 12A and B). For the HD patch, the model predicted high τ values on either sides of the bamboo patch, indicating that erosive trenches would develop along both sides of the patch. This effect of increased flow velocity and bed shear stress on either side of the patch was predicted to be less pronounced for the LD patch than for the HD patch. These model results agreed well with our field observations, showing erosive trenches at both sides of a patch for the HD bamboo patches (Figs. 2A, 3B and 4B), whereas no such erosive trenches were observed for the LD bamboo patches (Fig. 3B). Interestingly, natural *Spartina* tussocks had similar erosion trenches as found for the HD bamboo patches (Fig. 2A and B). The model was less successful in predicting the complete pattern of sedimentation and erosion along the main flow direction. That is, the model accurately predicted very low bed shear stress within and just behind the HD patch (Fig. 12B), which agreed with our flume (low stress levels; Fig. 9A–C) and field (sedimentation; Figs. 3A and 4A) observations. However, the model failed to predict the high stress levels at the leading edge of the HD patch (Fig. 12B), as we

Please cite this article as: Bouma, T.J., et al., Spatial flow and sedimentation patterns within patches of epibenthic structures, Continental Shelf Research (2007), doi:10.1016/j.csr.2005.12.019

observed in our flume (Fig. 9A–C) and field experiments (erosion; Figs. 3A and 4A). Within the LD patch, the model simulated elevated levels of bed shear stress (Fig. 12A). Although the flume measurements showed increased stress in the immediate vicinity of the canes (Fig. 9D–F), on the whole the levels were similar to, or even reduced, compared to the situation in front of the patch (Fig. 9G–I). This was in agreement with our field observations showing some small-scale erosion

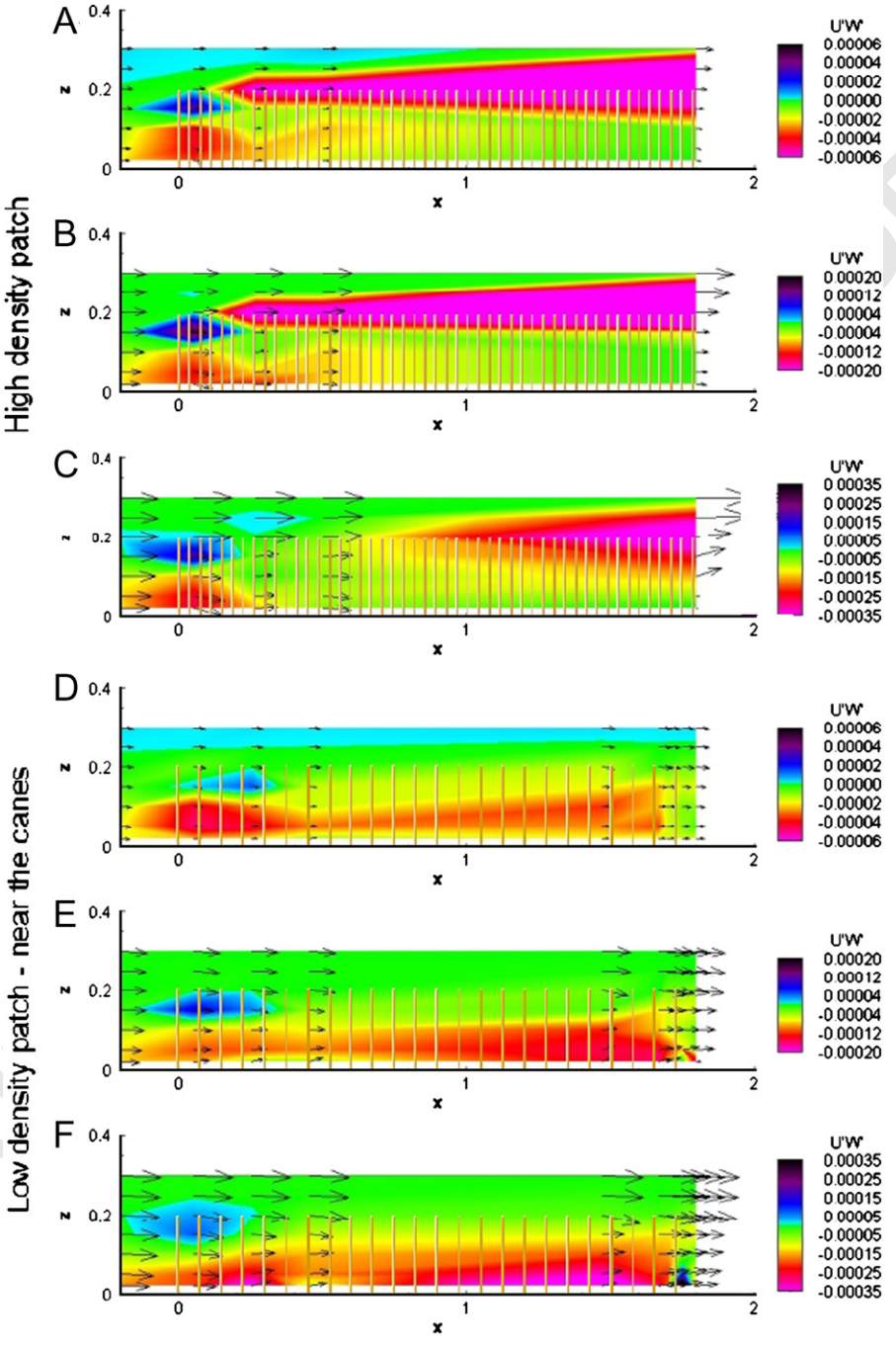

Fig. 9. (A–I) Profiles of vertical momentum flux ($\overline{u'w'}$; $m^2 s^{-2}$), measured at different positions in bamboo patches in the flume. Patch densities and velocities as in Fig. 7.

Please cite this article as: Bouma, T.J., et al., Spatial flow and sedimentation patterns within patches of epibenthic structures, Continental Shelf Research (2007), doi:10.1016/j.csr.2005.12.019

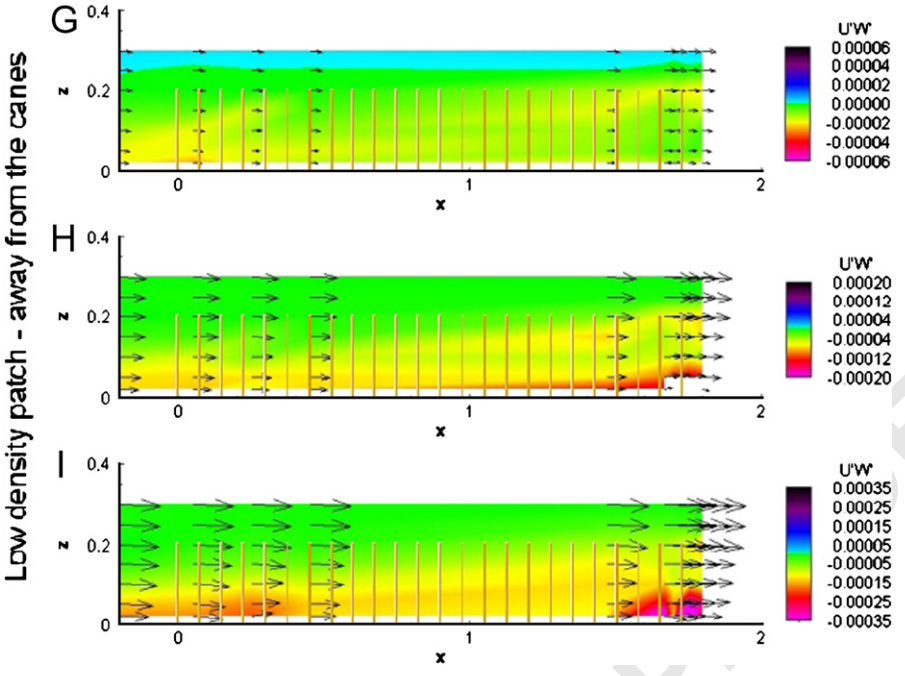

Fig. 9. (*Continued*)

directly adjacent to the canes in the LD patches, but no effect on the overall sedimentation in the LD patch (Fig. 3A).

4. Discussion

In the present study, we set out to: (1) identify spatial patterns of sedimentation and erosion that emerge within patches of epibenthic structures; and (2) assess the relevance of detailed hydrodynamic flume studies for understanding long-term sediment dynamics in such patches of epibenthic structures. The present study demonstrated that contrasting spatial patterns of sedimentation and erosion emerged within the HD and the LD patches, that these patterns were relatively independent of the sediment composition, and that these different patterns could be explained well by the hydrodynamic parameters obtained from our flume measurements. Our simulation results underlined the value of hydrodynamic models for up-scaling flume measurements and understanding spatially explicit sedimentation and erosion patterns in the field.

4.1. Effects of epibenthic structures on hydrodynamics and sediment dynamics

The growing appreciation of the ecological value of estuarine and coastal ecosystems combined with a growing awareness that physical models need to include biology to describe sedimentation patterns in these systems, has resulted in studies that address the effects of benthic organisms on hydrodynamics and sediment transport (for overviews see Allen, 2000; Koch, 2001; Widdows and Brinsley, 2002). The majority of the studies on epibenthic structures underline the importance of density for the effect on flow and resulting sediment transport near the bottom, regardless of whether these epibenthic structures originate from plants, animals or some kind of mimics (Bouma et al., 2005a; Friedrichs et al., 2000; Friedrichs, 2003). We are, however, not aware of studies that combine long-term field observations on sediment dynamics with detailed hydrodynamic descriptions obtained from flumes, so that most studies must infer data at one of these scales. In this respect, the present contribution offers a useful addition to the range of available studies, especially as we used hydrodynamic modelling for relating the flume and field data.

Please cite this article as: Bouma, T.J., et al., Spatial flow and sedimentation patterns within patches of epibenthic structures, Continental Shelf Research (2007), doi:10.1016/j.csr.2005.12.019

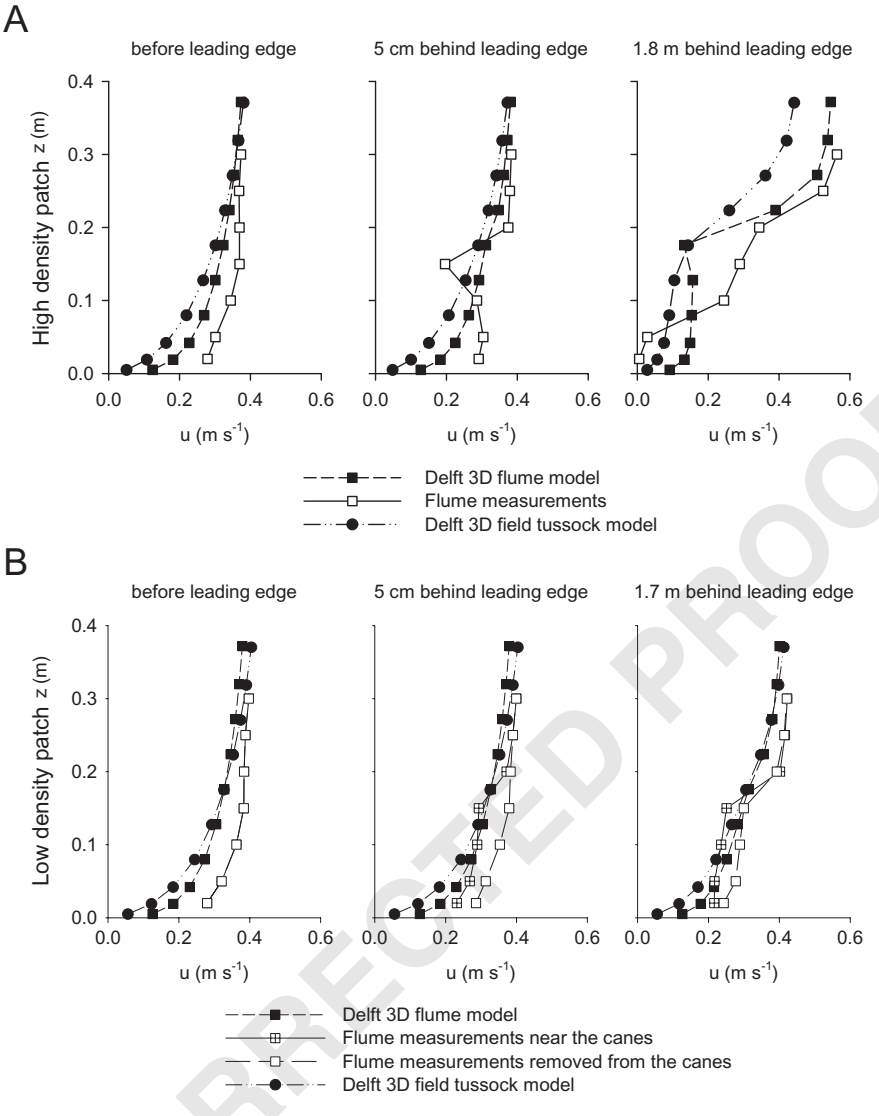

Fig. 10. Comparison of velocity profiles ($m\,s^{-1}$) in the HD patch (A) and LD patch (B) at different points in the canopy among Delft 3D model results from the flume, ADV measurements in the flume and Delft 3D model results from a bamboo tussock in the field.

In general terms, three flow conditions may be distinguished for flow over a bottom with epibenthic structures that intrude into the water column: *independent flow*, *interactive flow* and *skimming flow* (Vogel, 1994). Independent flow occurs if the spacing between the epibenthic structures greatly exceeds the height of the structure, causing the absence of interactions between the wake of neighbouring structures. This was obviously not the case in our HD or LD patches. Skimming flow occurs if the spacing between the epibenthic structures is $\leqslant$ the height of the structures, and if the total cover of the bottom by the roughness elements is $>1/12$. In true skimming flow over regularly spaced, equally high roughness elements, we can discern 3 flow regions: (1) boundary layer flow at some distance above the canopy; (2) a mixing layer around the top of the canopy; and (3) flow within the canopy that is dominated by Von Karman vortex structures from the wakes of the canes (Poggi et al., 2004). This is what we observed in the HD patch, even though the densities of roughness elements were on the low side for true skimming flow. The latter may explain why we see

Please cite this article as: Bouma, T.J., et al., Spatial flow and sedimentation patterns within patches of epibenthic structures, Continental Shelf Research (2007), doi:10.1016/j.csr.2005.12.019

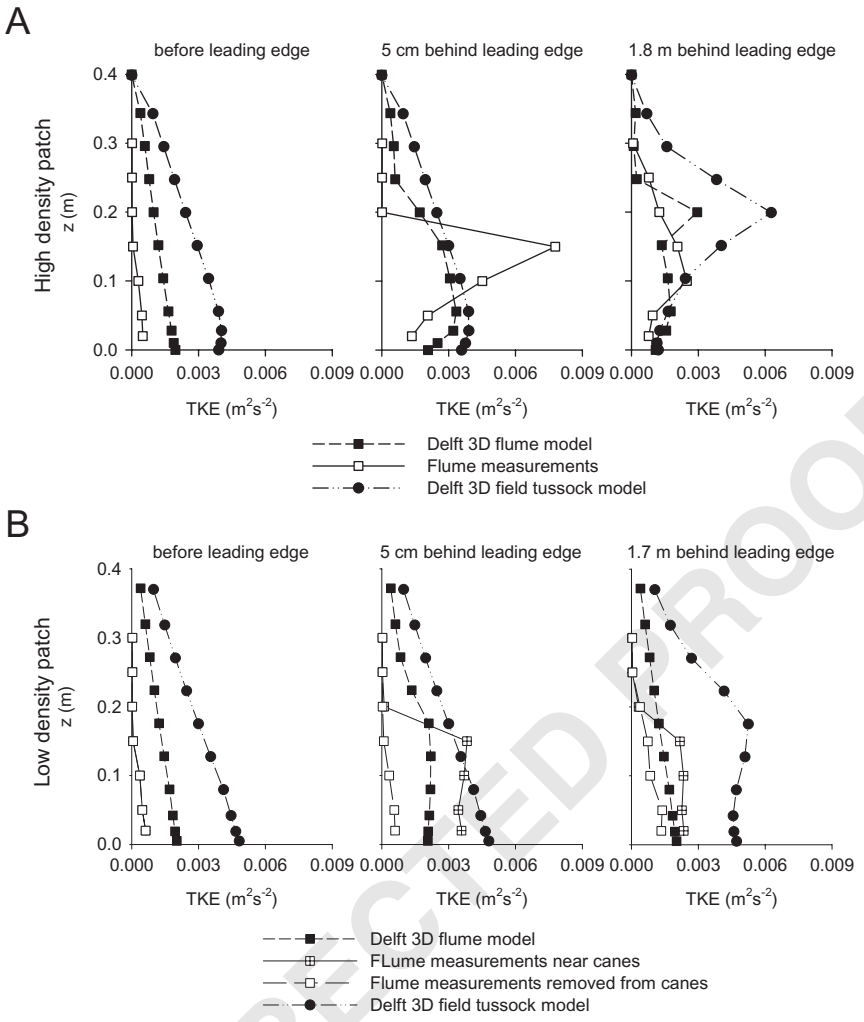

Fig. 11. Comparison of TKE ($m^2 s^{-2}$) profiles in the HD patch (A) and LD patch (B) at different points in the canopy among Delft 3D model results from the flume, ADV measurements in the flume and Delft 3D model results from a bamboo tussock in the field. Figures correspond to the velocity profiles in Fig. 10.

some increase in horizontal velocity from the bed to the top of the canopy. However, the vertical velocity gradient within the canopy at the HD was very low, which resulted in very low TKE and Reynolds stress levels inside the HD patch. As Reynolds stress is related directly to the force that water exerts on the bed, it is a useful predictor of areas of sedimentation and erosion. Indeed, the reduced Reynolds stress areas in our flume measurements and model simulations (inside the HD patch) are equivalent to areas where we observed sedimentation in our field patches. The areas where increased Reynolds stress occurred in our flume measurements (at the leading edge in the HD patches) or in the model simulations (lateral to the HD patches) equate to areas where we observed erosion in our HD field patches.

The velocity reduction by the bamboo structure, particularly in the HD patch, appears to be larger at higher velocities. This is almost certainly due to the fact that at the low flow settings, wake production inside the canopy was minimal. At element Reynolds numbers (Re_d) of <200, wake production is negligible, and turbulence production is reduced (Nepf, 1999). For our bamboo canes with a diameter of 8 mm this means that water needs to flow through the canopy with a speed of at least $0.02\,m\,s^{-1}$ for wakes to occur at all. At the lower

Please cite this article as: Bouma, T.J., et al., Spatial flow and sedimentation patterns within patches of epibenthic structures, Continental Shelf Research (2007), doi:10.1016/j.csr.2005.12.019

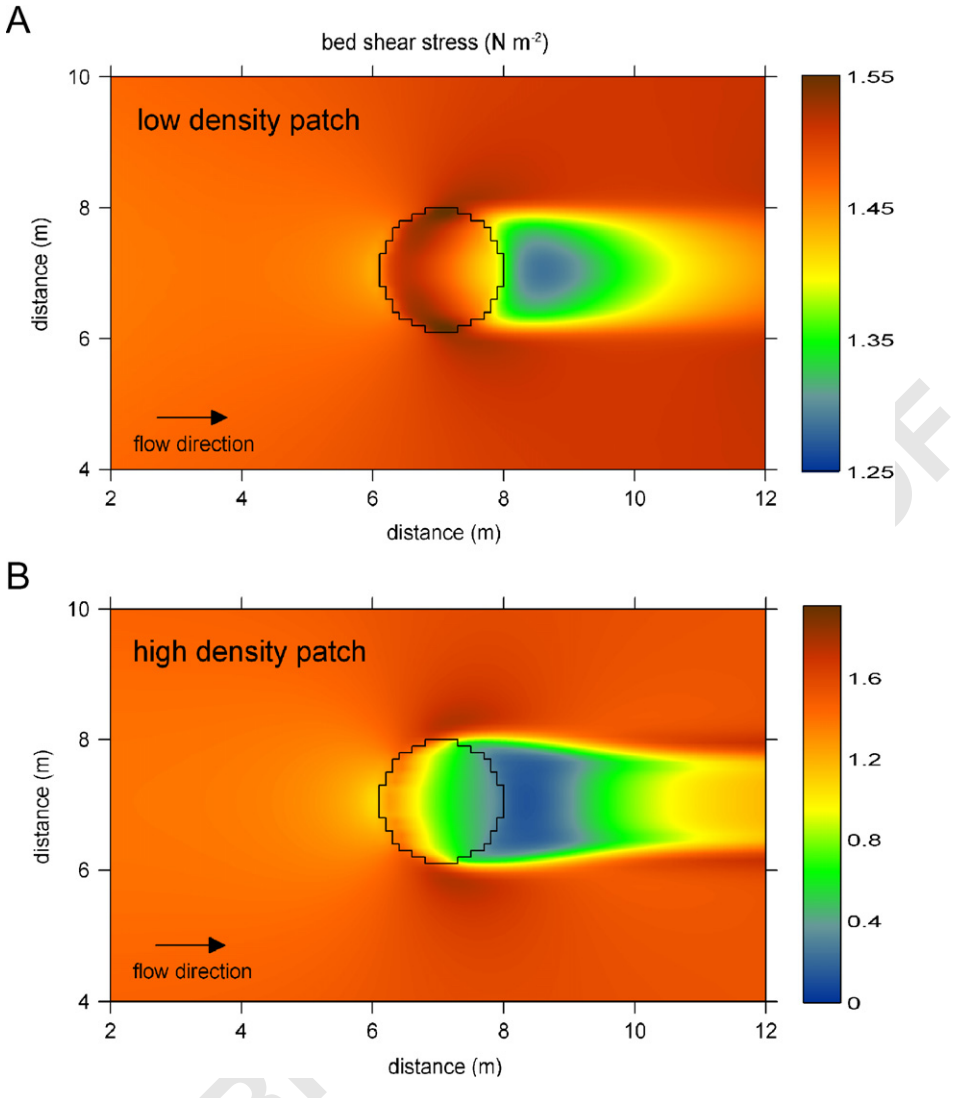

Fig. 12. Delft-3D simulated bottom shear stress ($N\,m^{-2}$) around a low (A) and high (B) density bamboo patch in the field. Note the difference in colour scale between (A) and (B).

velocity settings, flow inside the canopy was not far off this velocity, and flow reduction due to turbulence was therefore probably small. The higher velocities through the front part of the canopy will cause stronger wakes and hence much more momentum loss inside the canopy. This is illustrated very clearly in the TKE profiles of the HD patch. TKE reflects the balance between the increased turbulence intensity due to the effect of the wakes of the canes on one hand, and the reduced flow rate through the canopy on the other (Nepf, 1999). At the lower velocities, we still see a very strong elevation of TKE levels in the centre of the HD patch. At the highest velocity the TKE levels in the centre are much further reduced.

In the LD patch the measurements in close proximity to the canes showed similar patterns to the HD patch. In fact, TKE levels further inside the patch were higher in the LD canopy, due to the fact that flow velocity is much less reduced between the widely spaced canes. Due to the occurrence of a boundary layer at the bed, inside the canopy, stress levels at the bed close to the canes are high. The field observations show that in these areas erosion occurs. However these effects are very local.

Please cite this article as: Bouma, T.J., et al., Spatial flow and sedimentation patterns within patches of epibenthic structures, Continental Shelf Research (2007), doi:10.1016/j.csr.2005.12.019

In both the HD and LD patches, the regular alignment of the bamboo canes is expected to facilitate to some extent the flow between bamboo rows (White and Nepf, 2003). This effect is likely to have been stronger in the LD patch. A more natural, random distribution would have most likely resulted in a more patchy environment with small areas with strong local scour compared to areas with local deposition (Friedrichs et al., 2000).

4.2. Modelling as a tool for relating flume-hydrodynamics to field-sediment dynamics

Flow effects of epibenthic structures have been studied intensively using both natural structures such as mussel beds (Ackerman et al., 2001; van Duren et al., 2006), worm tubes, seagrass meadows (Koch, 2001; Madsen et al., 2001) or saltmarsh vegetation (Allen, 2000), as well as artificial structures (Bouma et al., 2005a; Friedrichs et al., 2000; Friedrichs, 2003; Nepf, 1999; Palmer et al., 2004; White and Nepf, 2003). Resulting data series have produced analytical and model formulations on hydrodynamics within patches of epibenthic structures (Nepf, 1999; Poggi et al., 2004, Uittenbogaard, unpublished results; White and Nepf, 2003). Present flume results on hydrodynamics agree well with the insights obtained from these analytical and model formulations, in the sense that these models also predict a strong density dependent reduction of bottom stress inside the canopy, areas of upward momentum transfer at the top of the leading edge of the canopy, and elevated stress at the bed at the leading edge of the patches (Uittenbogaard, unpublished results).

Our data also revealed a considerable spatial heterogeneity of hydrodynamic forcing on the bed inside the patches, leading to corresponding sedimentation and erosion patterns. The Delft-3D simulations accounted for the friction and turbulence that is generated by rigid cylindrical structures in the flow, which resulted in spatial differences in the flow structure inside the patches. Overall, these model results agreed reasonably well with both the flume and field observations, although some detailed flow phenomena were not reproduced accurately. In some cases, discrepancies might be ascribed to the model resolution, as our flume (and field) results may contain heterogeneity at a spatial scale smaller than the model resolution. For example, the relatively high shear in the LD patches generated by the model, most likely results from averaging flow effects from near the canes and further away. The greatest discrepancy between model and experimental results was observed at the leading edge inside a HD patch. Experimental data indicated high bottom shear and consequently high levels of erosion, whilst the model predicts a reduction in bottom shear stress throughout the patch. This indicates that the present model is a useful tool for studying the consequences of biophysical interactions, but that there is need for improving such models to deal accurately with leading edge effects.

Being able to model these relatively small-scale processes is especially important for understanding the landscape development in intertidal estuarine environments, as it is these small scale processes that determine initial colonisation. Models that incorrectly reproduce these leading edge effects, may still correctly describe what happens in large patches of epibenthic structures such as large patches of saltmarsh, but will be unsuitable for studying the processes that determine initial colonisation of unpopulated areas. In addition to affecting erosion and sedimentation, patches of epibenthic structures may also affect deposition of plant seeds and larvae of benthic animals. Although present hydrodynamic models may have some limitations for modelling aspects at the very fine scale, this study underlines strongly the value of modelling larger scale trends, and then relating flume and field data. Hence, the best way forward appears to be integrating field measurements, flume experiments, and modelling.

4.3. Scaling issues: vertical and horizontal dimensions and roughness density

Although our flume observations (and modelling exercises) provide adequate explanations for the sedimentation and erosion patterns we observed in the field, scaling remains an important aspect in relating flume measurements with field processes. Occurrence of skimming flow protects sediments from erosion, by lifting the boundary layer and displacing the high Reynolds stresses to an area higher up in the water column (Lopéz and Garcia, 1998). The ratio between the water column height and the height of the roughness structures (H/h) determines the extent to which skimming flow can occur (Nepf and Vivoni, 2000; Neumeier, this

Please cite this article as: Bouma, T.J., et al., Spatial flow and sedimentation patterns within patches of epibenthic structures, Continental Shelf Research (2007), doi:10.1016/j.csr.2005.12.019

volume). In the field, H/h will vary over the tidal cycle, whereas in a flume H is restricted by the flume dimensions (i.e. 0.4 m in the NIOO flume) and generally kept constant. If $H/h = 1$, the flow within vegetation is determined by the pressure gradient and the vegetative drag. In our artificial canopies this would mean a uniform drag throughout the water column, whereas for more heterogeneous biotic structures, the vertical profile will depend on the variation in vegetative drag. With an increase of H/h, the turbulent stress from the boundary layer above the canopy will start to contribute momentum to the flow inside the canopy. If $H/h \gg 10$ the flow will be completely dominated by vertical momentum exchange (Nepf and Vivoni, 2000).

In our flume experiments, we used $H/h = 2$ as we regarded the flows at this water height most important for the sedimentation patterns that occur in the field. That is, within a single tidal cycle, tidal currents tend to be strongest during upcoming and receding water, and lowest when the flood reaches its peak level (see Bouma et al., 2005b; note: the latter should not be confused with the linear relation between tidal amplitude and the maximum velocity reached in an individual tide). However, small changes in water depth will have a big impact on the H/h ratio and therefore on the momentum transfer within the canopy. Despite this possible source of error, hydrodynamic profiles in the flume appear to explain the sedimentation patterns in the field quite adequately.

The Delft 3D model predicted slightly different flow profiles for the bamboo patches in the flume compared with the field. This can be explained by the fact that in the field water may flow around a patchy structure, which is not possible in a 0.6 m wide flume. Simulations with the Delft 3D model indicate that this flow around patches develops when the patches do not fill the complete width of the model grid. This explains the difference between the flume simulations, where the patch completely fills the 0.6 m wide model grid so that water can only flow through and over the patch, and the field simulations where the water can flow around as well as through the patch. This difference will become increasingly important with increasing patch density, and may be expected to be more dominant in epibenthic structures, such as fully developed vegetation, relative to our bamboo patches. Hydrodynamic 3D models are valuable to assess the level of error that may be attributed to this kind of scaling artefact in flume studies. A limitation is due to a lack of full 3D hydrodynamic models that can cope with truly flexible roughness structures such as seagrasses.

Nowell and Church (1979) introduced the term roughness density (RD) to describe the fraction of the surface area that is covered by "epibenthic" structures. In our system, the bamboo canes had a diameter of 8.04 ± 0.13 mm ($n = 19$), which results in a RD of 0.020 for the HD patches (400 canes m^{-2}) and a RD of 0.00127 for the LD patches (25 canes m^{-2}). These RD values are relatively low when compared to some other studies. For example, Friedrichs et al. (2000) studied areas filled with round sticks (50 mm long; 5 mm diameter) with RD values ranging from 0.011 to 0.088. Despite the difference in RD values, the results of Friedrichs et al. (2000) and the present study revealed quite comparable general patterns with respect to sedimentation and hydrodynamics. The latter is in part explained by the effect of the ratio of the length of the structure to the distance between adjacent structures for the type of flow that occurs within a patch with epibenthic structures. Hence, this ratio will also be of major importance for the habitat modification that is induced by any kind of epibenthic structures. These modifications are referred to generally as ecosystem engineering (Jones et al., 1994, 1997; Reichman and Seabloom, 2002).

4.4. The role of epibenthic structures in ecosystem engineering

Ecosystem engineering has been found to affect significantly a broad range of ecosystems (Jones et al., 1994), and many ecosystem engineers may function as keystone species (Crooks, 2002). The latter certainly applies to organisms that produce epibenthic structures, regardless of whether they originate from benthic fauna (Callaway, 2003; Zuhlke, 2001) or flora (Bartholomew, 2002; Bologna and Heck, 2002; Hovel et al., 2002; Jenkins et al., 2002). The extent to which epibenthic structures are able to modify their habitat by reducing hydrodynamic energy will depend primarily on a combination of the density, stiffness and length or surface area of these structures (Bouma et al., 2005a; Gacia et al., 1999; Widdows and Brinsley, 2002). However, the costs to the organism will also increase with an increasing ability to modify hydrodynamic energy (Bouma et al., 2005a). The other factor determining the scope for ecosystem engineering is the average

Please cite this article as: Bouma, T.J., et al., Spatial flow and sedimentation patterns within patches of epibenthic structures, Continental Shelf Research (2007), doi:10.1016/j.csr.2005.12.019

flow rate. This will be relatively variable in highly dynamic environments, such as macro-tidal estuaries, and rather limited in more sheltered environments. This is indicated by the fact that we observed much stronger relative effects in the high velocity experiments in the flume.

Reduction of wave energy and/or current velocity enhances sediment accretion in sub- and intertidal vegetation, e.g. seagrass meadows and saltmarshes (Allen, 2000; Koch, 2001; Madsen et al., 2001; Palmer et al., 2004). Such sediment accretion may be beneficial to vegetation by: (a) enhancing nutrient availability in oligotrophic areas (Koch, 2001; Hemminga et al., 1998); (b) increasing light availability to submerged vegetation (Koch, 2001; Madsen et al., 2001); and (c) reducing inundation stress to intertidal saltmarsh species. The latter has been well documented for *Spartina,* where this process over time leads to the formation of dome shaped tussocks (Castellanos et al., 1994; Sanchez et al., 2001), and eventually affects the saltmarsh dynamics (van de Koppel et al., 2005).

The present study identifies two aspects that are related to ecosystem engineering, that deserve more attention. Firstly, the markedly different sediment dynamics between our eroding HD patches and nearby dome-shaped *Spartina* tussocks, once again demonstrates clearly the extent to which organism traits such as stiffness and shoot density are essential for the ecosystem engineering effects of an organism (Bouma et al., 2005a). Hence, it may be speculated that the organism traits which affect biophysical interactions are under evolutionary constraints (Bouma et al., 2005a; Odling-Smee et al., 2003). In addition to this ecological conclusion, the discrepancy in sedimentation patterns underlines the limitations of using mimics for understanding ecosystem engineering by real organisms. Although mimics may be highly relevant to identify general mechanisms (Bouma et al., 2005a), flume studies on mimics are unlikely to yield sufficient insight to model correctly a real ecosystem. Secondly, the spatial heterogeneity in sedimentation and hydrodynamics found in the present study, underlines the need for studying ecosystem engineering in a spatially explicit context. That is, the effect of an ecosystem engineer is likely to depend upon the size of its population, as well as the location within a patch. Whereas we observed high turbulence and erosion at the leading edge and the sides of a patch of epibenthic structures, strongly reduced velocities and resulting sedimentation were shown further down stream. This type of pattern may be typical for the configuration of sub- and intertidal vegetation such as *Spartina* tussocks. To understand the development of unpopulated areas towards colonised areas, there is thus a need for spatially explicit and scale-dependent knowledge of biophysical interactions of epibenthic structures.

5. Conclusions

Short-term flume studies can provide useful information on long-term sedimentation and erosion processes in the field provided that adequate spatial and hydrodynamical scaling is taken into consideration. We believe that modelling will offer a valuable tool to provide further insight in up-scaling flume observations to field measurements. However, hydrodynamic models require careful calibration with flume experiments. Our results underline the importance of quantifying spatial heterogeneity when studying small patches. This topic deserves more attention, regarding the importance for understanding the development of unpopulated areas towards colonised areas. The present study identifies the need for more spatially explicit and scale-dependent knowledge of biophysical interactions, both experimentally as well as from hydrodynamic modelling.

7. Uncited reference

Nepf et al., 1997.

Appendix

Sedimentation and erosion in the low density (LD) and the high density (HD) bamboo patches at the muddy (M) and the sandy (S) site of the Molenplaat. Elevation 0 indicates the height of the sediment before the bamboo patch was placed. The bamboo patch was present between −1 and 1 m distance along the *x*-axis. Data points represent the average over 3 replicate bamboo patches per treatment.

(See Fig. 13)

Please cite this article as: Bouma, T.J., et al., Spatial flow and sedimentation patterns within patches of epibenthic structures, Continental Shelf Research (2007), doi:10.1016/j.csr.2005.12.019

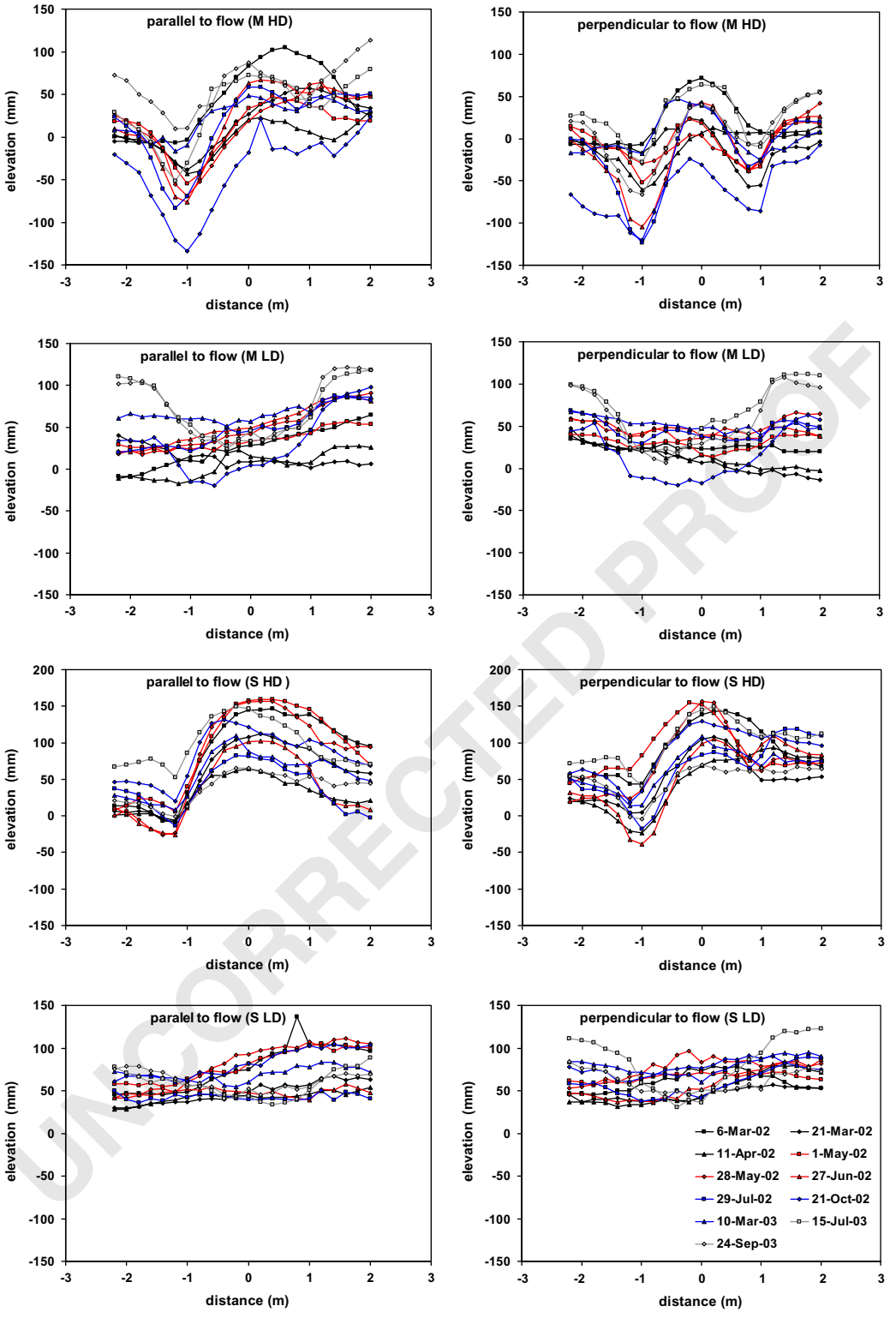

Fig. 13.

Please cite this article as: Bouma, T.J., et al., Spatial flow and sedimentation patterns within patches of epibenthic structures, Continental Shelf Research (2007), doi:10.1016/j.csr.2005.12.019

References

Abelson, A., Miloh, T., Loya, Y., 1993. Flow patterns induced by substrata and body morphologies of benthic organisms and their roles in determining availability of food particles. Limnology and Oceanography 38, 1116–1124.

Ackerman, J.D., Loewen, M.R., Hamblin, P.F., 2001. Benthic–Pelagic coupling over a zebra mussel reef in western Lake Erie. Limnology and Oceanography 46, 892–904.

Allen, J.R.L., 2000. Morphodynamics of Holocene salt marshes: a review sketch from the Atlantic and Southern North Sea coast of Europe. Quaternary Science Reviews 19, 1155–1231.

Baptist, M.J., unpublished results. A flume experiment on sediment transport with flexible, submerged vegetation. In: Abstract Volume, International Workshop on RIParian FORest Vegetated Channels: Hydraulic, Morphological and Ecological Aspects, 20–22 February 2003, Trento, Italy.

Bartholomew, A., 2002. Faunal colonization of artificial seagrass plots: the importance of surface area versus space size relative to body size. Estuaries 25, 1045–1052.

Blanchard, G.F., Sauriau, P.G., Cariou-Le Gall, V., Gouleau, D., Garet, M.J., Olivier, F., 1997. Kinetics of tidal resuspension of microbiota: testing the effects of sediment cohesiveness and bioturbation using flume experiments. Marine Ecology Progress Series 151, 17–25.

Bologna, P.A.X., Heck, K.L., 2002. Impact of habitat edges on density and secondary production of seagrass-associated fauna. Estuaries 25, 1033–1044.

Bouma, T.J., De Vries, M.B., Low, E., Peralta, G., Tánczos, I.C., van de Koppel, J., Herman, P.M.J., 2005a. Trade-offs related to ecosystem-engineering: a case study on stiffness of emerging macrophytes. Ecology 86, 2187–2199.

Bouma, T.J., De Vries, M.B., Low, E., Kusters, L., Herman, P.M.J., Tánczos, I.C., Hesselink, A., Temmerman, S., Meire, P., van Regenmortel, S., 2005b. Flow hydrodynamics on a mudflat and in salt marsh vegetation: identifying general relationships for habitat characterisations. Hydrobiologia 540, 259–274.

Callaway, R., 2003. Long-term effects of imitation polychaete tubes ion benthic fauna: they anchor *Mytilus edulis* (L.) banks. Journal of Experimental Marine Biology and Ecology 283, 115–132.

Castellanos, E.M., Figueroa, M.E., Davy, A.J., 1994. Nucleation and facilitation in salt-marsh succession—interactions between *Spartina maritima* and *Arthrocnemum perenne*. Journal of Ecology 82, 239–248.

Crooks, J.A., 2002. Characterizing ecosystem-level consequences of biological invasions: the role of ecosystem engineers. Oikos 97, 153–166.

De Leeuw, J., Apon, L.P., Herman, P.M.J., De Munck, W., Beeftink, W.G., 1992. Vegetation response to experimental and natural disturbances in 2 salt-marsh plant-communities in the Southwest Netherlands. Netherlands Journal of Sea Research 30, 279–288.

Friedrichs, M., 2003. Flow-induced effects of macrozoobenthic structures on the near-bed sediment transport. Ph.D. Thesis, University of Rostock, Germany, p. 80, unpublished.

Friedrichs, M., Graf, G., Springer, B., 2000. Skimming flow induced over a simulated polychaete tube lawn at low population densities. Marine Ecology Progress Series 192, 219–228.

Friend, P.L., Ciavola, P., Cappucci, S., Santos, R., 2003a. Bio-dependent bed parameters as a proxy tool for sediment stability in mixed habitat intertidal areas. Continental Shelf Research 23, 1899–1917.

Friend, P.L., Collins, M.B., Holligan, P.M., 2003b. Day-night variation of intertidal flat sediment properties in relation to sediment stability. Estuarine Coastal and Shelf Science 58, 663–675.

Gacia, E., Granata, T.C., Duarte, C.M., 1999. An approach to measurement of particle flux and sediment retention within seagrass (*Posidonia oceanica*) meadows. Aquatic Botany 65, 255–268.

Hemminga, M.A., van Soelen, J., Maas, Y.E.M., 1998. Biomass production in pioneer *Spartina anglica* patches: evidence for the importance of seston particle deposition. Estuarine Coastal and Shelf Science 47, 797–805.

Hendriks, I.E., van Duren, L.A., Herman, P.M.J., 2006. Turbulence levels in a flume compared to the field. Journal of Sea Research 55, 15–29.

Herman, P.M.J., Middelburg, J.J., Heip, C.H.R., 2001. Benthic community structure and sediment processes on an intertidal flat: results from the ECOFLAT project. Continental Shelf Research 21, 2055–2071.

Houwing, E.J., 2000. Morphodynamic development of intertidal mudflats: consequences for the extension of the pioneer zone. Continental Shelf Research 20, 1735–1748.

Hovel, K.A., Fonseca, M.S., Myer, D.L., Kenworthy, W.J., Whitfield, P.E., 2002. Effects of seagrass landscape structure, structural complexity and hydrodynamic regime on macrofaunal densities in North Carolina seagrass beds. Marine Ecology Progress Series 243, 11–24.

Jenkins, G.P., Walker-Smith, G.K., Hamer, P.A., 2002. Elements of habitat complexity that influence harpacticoid cocepods associated with seagrass beds in a temperate bay. Oecologia 131, 598–605.

Jones, C.G., Lawton, J.H., Shachak, M., 1994. Organisms as ecosystem engineers. Oikos 69, 373–386.

Jones, C.G., Lawton, J.H., Shachak, M., 1997. Positive and negative effects of organisms as physical ecosystem engineers. Ecology 78, 1946–1957.

Kim, S.C., Friedrichs, C.T., Maa, J.P.Y., Wright, L.D., 2000. Estimating bottom stress in tidal boundary layer from Acoustic Doppler Velocimeter data. Journal of Hydraulic Engineering 126, 399–406.

Koch, E.W., 1999. Sediment resuspension in a shallow *Thalassia testudinum* bank ex Konig bed. Aquatic Botany 65, 269–280.

Koch, E.W., 2001. Beyond light: physical, geological, and geochemical parameters as possible submersed aquatic vegetation habitat requirements. Estuaries 24, 1–17.

Koch, E.W., Gust, G., 1999. Water flow in tide- and wave-dominated beds of the seagrass *Thalassia testudinum*. Marine Ecology Progress Series 184, 63–72.

Lesser, G., Roelvink, J., van Kester, J., Stelling, G., 2004. Development and validation of a three-dimensional morphological model. Coastal Engineering 51, 883–915.

Leonard, L.A., Luther, M.E., 1995. Flow hydrodynamics in tidal marsh canopies. Limnology and Oceanography 40, 1474–1484.

Lopéz, F., Garcia, M., 1998. Open-channel flow through simulated vegetation: Suspended sediment transport modeling. Water Resources Research 34, 2341–2352.

Please cite this article as: Bouma, T.J., et al., Spatial flow and sedimentation patterns within patches of epibenthic structures, Continental Shelf Research (2007), doi:10.1016/j.csr.2005.12.019

Madsen, J.D., Chambers, P.A., James, W.F., Koch, E.W., Westlake, D.F., 2001. The interaction between water movement, sediment dynamics and submersed macrophytes. Hydrobiologia 444, 71–84.

Nepf, H.M., 1999. Drag, turbulence, and diffusion in flow through emergent vegetation. Water Resource Research 35, 479–489.

Nepf, H.M., Vivoni, E.R., 2000. Flow structure in depth-limited, vegetated flow. Journal of Geophysical Research-Oceans 105, 28547–28557.

Nepf, H.M., Sullivan, J.A., Zavistoski, R.A., 1997. A model for diffusion within emergent vegetation. Limnology and Oceanography 42, 1735–1745.

Neumeier, U., Ciavola, P., 2004. Flow resistance and associated sedimentary processes in a *Spartina maritima* salt-marsh. Journal of Coastal Research 20, 435–447.

Nowell, A.R.M., Church, M., 1979. Turbulence flow in a depth-limited boundary layer. Journal of Geophysical Research 84, 4816–4824.

Odling-Smee, F.J., Laland, K.N., Feldman, M.W., 2003. Niche Construction; the Neglected Process in Evolution. Princeton University Press, Princeton, NJ, USA.

Palmer, M.R., Nepf, H., Petterson, J.R., Ackerman, J.D., 2004. Observations of particle capture on a cylindrical collector: implications for particle accumulation and removal in aquatic systems. Limnology and Oceanography 49, 76–85.

Paterson, D.M., 1989. Short-term changes in the erodability of intertidal cohesive sediments related to the migratory behavior of epipelic diatoms. Limnology and Oceanography 34, 223–234.

Paterson, D.M., Tolhurst, T.J., Kelly, J.A., Honeywill, C., de Deckere, E.M.G.T., Huet, V., Shayler, S.A., Black, K.S., de Brouwer, J., Davidson, I., 2000. Variations in sediment properties, Skeffling mudflat, Humber Estuary, UK. Continental Shelf Research 20, 1373–1396.

Poggi, D., Porporato, A., Ridolfi, L., Albertson, J.D., Katul, G.G., 2004. The effect of vegetation density on canopy sub-layer turbulence. Boundary-Layer Meteorology 111, 565–587.

Reichman, O.J., Seabloom, E.W., 2002. The role of pocket gophers as subterranean ecosystem engineers. Trends in Ecology and Evolution 17, 44–49.

Sanchez, J.M., SanLeon, D.G., Izco, J., 2001. Primary colonisation of mudflat estuaries by *Spartina maritima* (Curtis) Fernald in Northwest Spain: vegetation structure and sediment accretion. Aquatic Botany 69, 15–25.

Shi, Z., Hamilton, L.J., Wolanski, E., 2000. Near-bed currents and suspended sediment transport in saltmarsh canopies. Journal of Coastal Research 16, 909–914.

Steyaert, M., Herman, P.M.J., Moens, T., Widdows, J., Vincx, M., 2001. Tidal migration of nematodes on an estuarine tidal flat (the Molenplaat, Schelde Estuary, SW Netherlands). Marine Ecology Progress Series 224, 299–304.

Temmerman, S., Govers, G., Meire, P., Wartel, S., 2003. Modelling long-term tidal marsh growth under changing tidal conditions and suspended sediment concentrations, Scheldt estuary, Belgium. Marine Geology 193, 151–169.

Temmerman, S., Govers, G., Wartel, S., Meire, P., 2004. Modelling estuarine variations in tidal marsh sedimentation: response to changing sea level and suspended sediment concentrations. Marine Geology 212, 1–19.

Temmerman, S., Bouma, T.J., Govers, G., Wang, Z.B., De Vries, M.B., Herman, P.M.J., 2005. Impact of vegetation on flow routing and sedimentation patterns: three-dimensional modeling for a tidal marsh. Journal of Geophysical Research 110, F04019.

Tolhurst, T.J., Black, K.S., Shayler, S.A., Mather, S., Black, I., Baker, K., Paterson, D.M., 1999. Measuring the in situ erosion shear stress of intertidal sediments with the cohesive strength meter (CSM). Estuarine Coastal and Shelf Science 49, 281–294.

Tolhurst, T.J., Riethmuller, R., Paterson, D.M., 2000a. In situ versus laboratory analysis of sediment stability from intertidal mudflats. Continental Shelf Research 20, 1317–1334.

Tolhurst, T.J., Black, K.S., Paterson, D.M., Mitchener, H.J., Termaat, G.R., Shayler, S.A., 2000b. A comparison and measurement standardisation of four in situ devices for determining the erosion shear stress of intertidal sediments. Continental Shelf Research 20, 1397–1418.

Thompson, C.E.L., Amos, C.L., Jones, T.E.R., Chaplin, J., 2003. The manifestation of fluid-transmitted bed shear stress in a smooth annular flume—a comparison of methods. Journal of Coastal Research 19, 1094–1103.

Uittenbogaard, R.E., unpublished results. Modelling turbulence in vegetated aquatic flows. In: Abstract Volume, International Workshop on RIParian FORest Vegetated Channels: Hydraulic, Morphological and Ecological Aspects, 20–22 February 2003, Trento, Italy.

van de Koppel, J., van der Wal, D., Bakker, J.P., Herman, P.M.J., 2005. Self-organization and vegetation collapse in salt marsh ecosystems. American Naturalist 165, E1–E12.

van der Wal, D., Pye, K., 2004. Patterns, rates and possible causes of saltmarsh erosion in the Greater Thames area (UK). Geomorphology 61, 373–391.

van der Wal, D., Pye, K., Neal, A., 2002. Long-term morphological change in the Ribble Estuary, northwest England. Marine Geology 189, 249–266.

van Duren, L.A., Herman, P.M.J., Sandee, A.J.J., Heip, C.H.R., 2006. Effects of mussel filtering activity on boundary layer structure. Journal of Sea Research 55, 3–14.

van Katwijk, M.M., Hermus, D.C.R., 2000. Effects of water dynamics on *Zostera marina*: transplantation experiments in the intertidal Dutch Wadden Sea. Marine Ecology Progress Series 208, 107–118.

Vogel, S., 1994. Life in Moving Fluids; the Physical Biology of Flow. Princeton University Press, Princeton, NJ, USA.

White, B.L., Nepf, H.M., 2003. Scalar transport in random cylinder arrays at moderate Reynolds numbers. Journal of Fluid Mechanics 487, 43–79.

Widdows, J., Brinsley, M., 2002. Impact of biotic and abiotic processes on sediment dynamics and the consequences to the structure and functioning of the intertidal zone. Journal of Sea Research 48, 143–156.

Widdows, J., Blauw, A., Heip, C.H.R., Herman, P.M.J., Lucas, C.H., Middelburg, J.J., Schmidt, S., Brinsley, M.D., Twisk, F., Verbeek, H., 2004. Role of physical and biological processes in sediment dynamics of a tidal flat in Westerschelde Estuary, SW Netherlands. Marine Ecology Progress Series 274, 41–56.

WL|Delft Hydraulics, 2003. User manual Delft-3D FLOW, WL|Delft Hydraulics (www.wldelft.nl), Delft, The Netherlands.

Wright, L.D., Friedrichs, C.T., Hepworth, D.A., 1997. Effects of benthic biology on bottom boundary layer processes, Dry Tortugas Bank, Florida Keys. Geo-Marine Letters 17, 291–298.

Please cite this article as: Bouma, T.J., et al., Spatial flow and sedimentation patterns within patches of epibenthic structures, Continental Shelf Research (2007), doi:10.1016/j.csr.2005.12.019

Ysebaert, T., Meire, P., Herman, P.M.J., Verbeek, H., 2002. Macrobenthic species response surfaces along estuarine gradients: prediction by logistic regression. Marine Ecology Progress Series 225, 79–95.

Zuhlke, R., 2001. Polychaete tubes create ephemeral community patterns: Lanice conchilega (Pallas, 1766) associations studied over six years. Journal of Sea Research 46, 261–272.

Please cite this article as: Bouma, T.J., et al., Spatial flow and sedimentation patterns within patches of epibenthic structures, Continental Shelf Research (2007), doi:10.1016/j.csr.2005.12.019